universität wien

# MASTERARBEIT

Titel der Masterarbeit

„Dissecting small RNA silencing pathways in mouse embryonic stem cells“

verfasst von

Fabian Braukmann

angestrebter akademischer Grad

Master of Science (MSc)

Wien, 2013

| | | |
|---|---|---|
| Studienkennzahl Studienblatt: | lt. | A 066 834 |
| Studienrichtung Studienblatt: | lt. | Masterstudium Molekulare Biologie UG2002 |
| Betreut von: | | Dr. Stefan Ludwig Ameres |

## Abstract

MicroRNAs (miRNAs) regulate the expression of genes at the post-transcriptional level, ensuring normal development and physiology. Much of what is known about the genetic composition of small RNA pathways in mammals is inferred from genetic screens performed in model organisms, such as flies and worms. The recent generation of haploid mouse embryonic stem-cells (mESCs) enables us to directly address the genetic requirements for murine small RNA pathways. As a proof-of-principle for such a screen, we initially characterize a mESC line bearing an enhanced gene-trap insertion in the *Drosha* gene, fortuitously isolated from random retroviral mutagenesis of haploid mESCs.

The analysis of the *Drosha* mutant mESCs revealed changes in *Drosha* gene products and miRNA profile. The mutagenesis approach results in a ~100 fold decrease in *drosha* mRNA levels, rendering the protein undetectable in Western blot analysis. Moreover *Drosha* mutant mESCs recapitulate post-transcriptional cross-regulation between Drosha and its double-stranded RNA binding partner DGCR8, resulting in elevated *dgcr8* mRNA levels; and the global decrease in small RNA levels affects Argonaute 2 protein stability, while mRNA levels are increased. The systematic analysis of constructs reporting either on endogenous or artificial small RNA-mediated gene regulation in *Drosha* mutant mESCs evaluates different strategies to establish a screening system for the genetic requirements of small RNA-mediated gene regulation in mESCs.

Together, our results show that haploid mESCs combined with enhanced gene-trap mutagenesis allows identifying and characterizing core components of the miRNA pathway in a genetic screen. The generated mutants validate important molecular and biological functions of small RNA-mediated gene silencing. Finally, we propose strategies for the systematic identification of novel miRNA pathway components in a genetic screen.

# Zusammenfassung

MicroRNAs (miRNAs) regulieren Genexpression auf der post-transkriptionalen Ebene und garantieren reguläre Entwicklung und Physiologie. Genetische Screening-Studien im Fadenwurm und der Fruchtfliege haben zu dem Verständnis des kleinen RNA Genregulationsweg in Säugetieren beigetragen. Die jüngste Entwicklung von haploiden maus-embryonalen Stammzellen (mESCs) ermöglicht uns die genetischen Anforderungen dieses Genregulationswegs direkt in Mäusen zu bestimmen. Die Möglichkeit, Mutanten des kleinen RNA Genregulationsweg in einer Screening-Studie zu generieren wird durch die Charakterisierung einer exemplarischen mESC-Linie überprüft. Diese entstand in einer zufällig screening Studie, in welcher ein retrovirales Konstrukt zufällig eine verbesserte Genfalle innerhalb des *Drosha* Gens integrierte (*Drosha*-mutierte mESCs) wurde. Des Weiteren testete ich Reporterkonstrukte um eine selektive screening-Studie für die genetischen Anforderungen in mECS zu ermöglichen.

Die Analyse von *Drosha*-mutierten mESCs zeigt, dass die Mutagenese-Methode sowohl *Droshas* mRNA- und Proteinkonzentration als auch die Konzentration von kanonische miRNAs verringert. Zusätzlich konnte die gegenseitige Regulation von *Drosha* und *DGCR8* rekapituliert werden. Die systematische Analyse zweier Konstrukte, welche die Generegulation von kleinen RNAs offenbarten, ermöglicht die Entwicklung von verbesserten screening Strategien in mESC.

Diese Resultate zeigen, dass haploide mESCs und die verbesserte Genfalle die Identifikation und Charakterisierung von Mutanten des kleinen RNA Genregulationsweg ermöglichen und die generierten Mutanten molekulare und biologische Funktionen rekapitulieren. Außerdem schlagen wir eine Möglichkeit vor, um eine selektive screening Studie für Komponenten des kleinen RNA Genregulationsweg durchzuführen.

Abstract ..... 3

Zusammenfassung ..... 4

1 Introduction ..... 7

1.1 microRNAs ..... 7

1.2 Forward genetic screens ..... 18

1.3 Project Outline ..... 21

2 Results ..... 23

2.1 Characterization of *Drosha* mutant mESCs ..... 23

2.2 Design of a reporter-based screen to identify the genetic requirements for small RNA-mediated gene regulation in mESCs ..... 33

3 Discussion ..... 43

4 Experimental procedures ..... 48

Bibliography ..... 62

Acknowlegement ..... 72

Curriculum Vitae ..... 73

Supplements ..... 74

# 1 Introduction

## 1.1 microRNAs

### Discovery of microRNAs

In 1993 the laboratories of Victor Ambros and Gary Ruvkun identified a new mechanism of gene regulation in *C. elegans,* which is based on a small, ~22 nucleotide (nt) RNA (Lee et al., 1993; Wightman et al., 1993). This seminal discovery revealed that the gene *lin-4*, which is required for normal developmental timing in worms, produces two short RNAs of 22 and 61 nucleotides (nts), respectively. The longer form was later established as a precursor of the shorter RNA. The shorter form exhibits complementarity to sites in the 3'UTR of the *lin-14* mRNA. Wightman *et. al* already suggested that the gene product of *lin-4* regulates *lin-14* post-transcriptionally to coordinate developmental timing, hence, representing the first example for a novel class of small gene-regulatory RNAs, which later became famous as microRNAs (Wightman et al., 1993). But the boom around small RNAs as gene regulatory molecules only really began, when the gene *let-7*, likewise discovered in a genetic screen for heterochronic genes in *C. elegans*, was also described to produce a small RNA (Reinhart et al., 2000). But in contrast to *lin-4*, *let*-7 is conserved in flies, mice and humans. Subsequent small RNA sequencing approaches identified dozens of small RNAs in worms, flies and humans (Lagos-Quintana et al., 2001; Lau et al., 2001; Lee and Ambros, 2001). Meanwhile, the primary repository for miRNA sequences and annotations – miRbase – reports more than 24,500 miRNAs in animals, plants and viruses (Griffiths-Jones, 2004). Today, miRNAs are well established as key regulators of organismal development, physiology and disease (Bartel, 2004); and together with other classes of small RNAs they regulate some aspect of nearly every conceivable biological process (Ghildiyal and Zamore, 2009).

## Origin and classification of small RNAs

In animals, three classes of small RNAs have been described: MicroRNAs (miRNAs), small interfering RNAs (siRNAs) and PIWI-associated RNAs (piRNAs) (Aravin et al., 2006; Brennecke et al., 2007; Czech et al., 2008; Ghildiyal et al., 2008; Okamura et al., 2008). Their biogenesis and the associated effector Argonaute (Ago) protein distinguish the three small RNA classes: PIWI-associated RNAs derive from single-stranded RNA precursors and associate with the PIWI subfamily of Argonaute proteins. They are mainly restricted to the germline of flies and mammals where they defend the genome against mobile genetic elements, such as transposons (Brennecke et al., 2007; Girard et al., 2006). MicroRNAs as well as siRNAs derive from double-stranded RNA precursors, bind to the Ago-clade of the Argonaute protein family and are thought to be ubiquitously expressed. Small interfering RNAs originate from viral dsRNA replication intermediates, experimentally introduced long dsRNA (exo-siRNAs) or endogenous long dsRNA (endo-siRNAs) encoded in the genome (Mello and Conte, 2004; Watanabe et al., 2008). MicroRNAs are encoded in the genome of animals and plants, and play crucial roles in the regulation of organismal development and physiology. The differences in plant and animal miRNA biogenesis, gene organization and target recognition as well as the absence of miRNAs in fungi suggest that the miRNA pathway evolved at least twice (Axtell et al., 2011).

## MicroRNA biogenesis

MicroRNAs are encoded in the intron of protein-coding genes or as independent transcription units and are transcribed by RNA Polymerase II as capped and polyadenylated primary miRNA (pri-miRNA) transcripts (Baskerville and Bartel, 2005; Lee et al., 2004a; Wang et al., 2008). The transcript length ranges from several hundred up to several kilobases and can contain multiple miRNA-

encoding hairpins (Lee et al., 2002; Yekta et al., 2004). Primary miRNAs are initially recognized and processed by the nuclear RNAse III enzyme Drosha, which acts together with its double-stranded RNA binding protein partner DGCR8 to excise a ~ 60 nt long precursor-miRNA (pre-miRNA) hairpin (Han et al., 2006; Kim and Kim, 2007; Lee et al., 2003). DGCR8 recognizes the single strand/stem junction of the pri-miRNA (Han et al., 2004). Drosha/DGCR8 forms the core of an ~600 kDa complex referred to as the microprocessor (Denli et al., 2004; Gregory et al., 2004). Processing of some pri-miRNAs is enhanced by primary sequence motives: For example, the splicing regulator SRp20/SRSF3 (Huang and Steitz, 2001), recognizes a CNNC motive and increases the efficiency of pri-miRNA processing (Auyeung et al., 2013). Furthermore, the microprocessor consists of numerous cofactors, such as DEAD-box and DEAH-box family RNA helicases, heterogeneous nuclear ribonucleo-proteins (hnRNPs) and the Ewing's sarcoma family of proteins containing an RNA recognition motif (RRM) and a zinc-finger domain that may fine-tune pre-miRNA processing specificity or efficiency (Gregory et al., 2004; Mathonnet et al., 2007). After Drosha-mediated pri-miRNA processing, the resulting pre-miRNA is recognized by Exportin-5 and transported in a Ran-GTP-dependent manner into the cytoplasm (Braun et al., 2011; Eystathioy et al., 2003; Okada et al., 2009).

In the cytoplasm a second RNase III enzyme, Dicer, cleaves the pre-miRNA and generates a ~22 nt mature miRNA duplex (Zhang et al., 2004). Dicer is a multi-domain protein and identifies its substrate by protein domains, which recognize specific structural features of pre-miRNAs (MacRae et al., 2006): Studies in *Giardia intestinalis* showed that the PAZ domain of Dicer is able to bind the 3' ends of RNA (MacRae et al., 2007). In humans, PAZ-domain-mediated pre-miRNA recognition is supported by a 5' pocket recognizing the 5' end of the pre-miRNA. Cleavage occurs 22 nucleotides from the 5' end (Park et al., 2011). In mammals two dsRNA binding proteins, PACT and TRBP, partner with Dicer and are required for efficient miRNA biogenesis (Lee et al., 2006).

The Dicer products, ~22 nt short dsRNAs, are assembled into Argonaute proteins and one of the two stranded – the guide strand – is loaded (Kawamata and Tomari, 2010). Hsp90 chaperone is suggested to promote Argonaute loading (Johnston et al., 2010). Guide strand selection depends mainly on the thermodynamic properties at the 5' end of the miRNA duplex; the released strand is called passenger strand and, once expelled, is rapidly degraded (Iwasaki et al., 2010; Schwarz et al., 2003). The guide strand guides Argonaute proteins to complementary regions typically located in the 3´ UTR of messenger RNAs (mRNAs) to direct post-transcriptional gene regulation (Fabian et al., 2010).

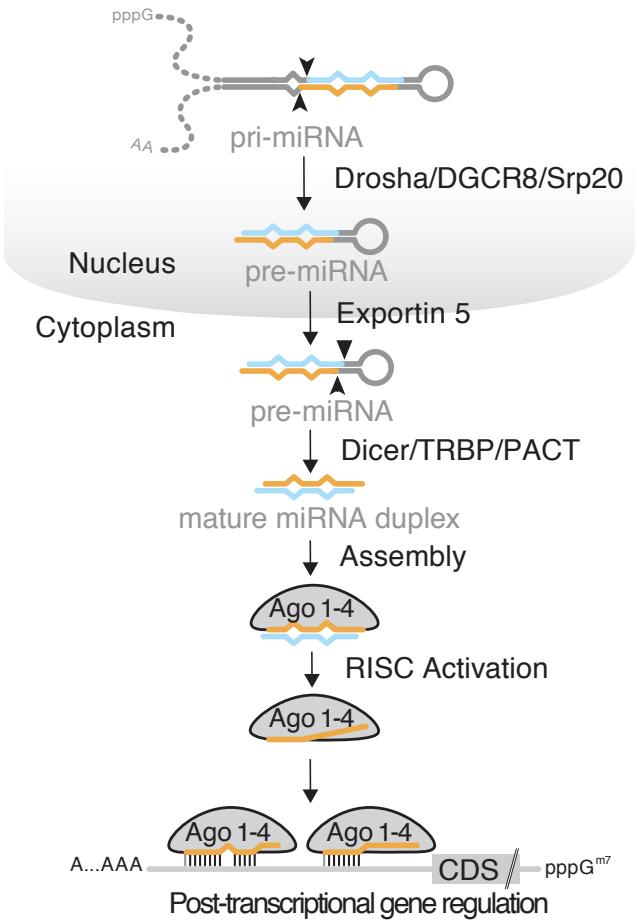


**Figure 1.1 miRNA biogenesis pathway.** miRNAs genes are transcribed by RNA polymerase II. Drosha/DiGeorge syndrome critical region gene 8 (DGCR8)/SRp20 process the primary miRNA transcripts and generate a ~60nt long precursor miRNA (pre-miRNA). Exportin-5 exports the pre-miRNA from the nucleus into the cytoplasm. The Dicer/TRBP/PACT complex cleaves the pre-miRNA and generates a mature miRNA duplex that is assembled into the Argonaute. After second strand removal the active RNA-induced silencing complex (RISC) is formed. The remaining miRNA strand guides RISC to the target mRNA and regulate gene expression.

### Non-canonical miRNA biogenesis

Beside canonical miRNA biogenesis mediated by the two RNAse III enzymes Drosha and Dicer, a small number of miRNAs are generated by mechanisms that bypass one of the two RNAse III enzyme (Yang and Lai, 2011).

Mirtrons are an example for this phenomenon, initially described in worms and flies. They derived from short introns which directly gives rise to pre-miRNAs without a requirement for Drosha-mediated processing (Westholm and Lai, 2011). The splicing machinery excises the intron and forms a branched lariat structure (Okamura et al., 2007). In the subsequent step the lariat debranching enzyme processes the short intron and generates a pre-miRNA-like structure that is processed by Dicer in the cytoplasm (Ruby et al., 2007). Mitrons were also discovered in mammals (Berezikov et al., 2007). Here they can derive as well from the 5' or 3' end of long intron (Babiarz et al., 2008). In this case an additional processing step occurs and only one end of the pre-miRNA is defined by the splicing event. The second end is generated by either the RNA exosome, the major 3′ → 5′ exonuclease complex for 3' tailed mirtrons; for 5' tailed mirtrons processing by the 5′ → 3′ exonucleases XRN1 and XRN2 is suggested (Westholm and Lai, 2011).

Small nucleolar RNAs (snoRNAs) are conserved short RNAs that function as guide molecules for posttranscriptional modification of ribosomal and small nuclear RNA (rRNA and snRNA). Based on conserved sequence elements snoRNAs are classified as C/D box-snoRNAs, guiding methylation, and H/ACA-snoRNAs, guiding pseudouridylation (Kiss, 2002). *Giardia lamblia*, a flagellated protozoan parasite causing giardiasis, expresses Dicer-dependent functional snoRNA-derived RNAs (sdRNAs) (Saraiya and Wang, 2008). Subsequently small RNAs derived from the box-C/D and box-H/ACA-snoRNAs families were found in animals and plants (Taft et al., 2009). A regulatory potential was observed in a reporter assay using perfectly complementary binding site, suggesting that

sdRNAs are abundant enough to regulate gene-expression (Brameier et al., 2011).

Transfer RNAs (tRNAs) are RNA polymerase III transcripts and deliver amino acid to the protein synthesis machinery (Giegé, 2008). Some tRNAs can exist in two energetically similar conformations, the characteristic cloverleaf structure or a hairpin-like structure, which resembles a Dicer substrate (Phizicky and Hopper, 2010). Small RNA deep-sequencing experiments In mouse embryonic stem-cells (mESCs) revealed that small RNAs can be produced from tRNAs. These tRNA-derived RNAs (tdRNAs) were DGCR8 independent and Dicer dependent, suggesting an alternative miRNA source (Babiarz et al., 2008). Subsequently, additional tdRNAs were identified in humans, where modest regulatory competence was shown (Haussecker et al., 2010).

tRNAseZ processes the 3' end of tRNA precourser (pre-tRNA) and releases a 3' trail (Phizicky and Hopper, 2010). Another type of tdRNAs are tRNaseZ-derived miRNAs. They accumulate independently of tRNA-maturation and therefore might play a role in gene expression regulation (Lee et al., 2009). In murin-ɣ-herpes-virus 68 (MHV68) RNA polymerase III transcripts are processed in a Drosha-independency but tRNaseZ/Dicer dependency manner (Bogerd et al., 2010), but their biological function remains unclear.

Endogenous short hairpin RNAs (endo-shRNAs), like the miR-320 were found in mESCs. In regular small RNA cloning protocols, the 3p species abundance of miR-320 dominates the 5p species. Inefficient small RNA cloning of the 5p species could cause the unbalanced distribution. RNA polymerase III generates 5'-triphosphate ends that cannot be ligated to the 5' adaptor in regular small RNA cloning protocols. Deep-sequencing data from *DGCR8* and *Dicer* mutant mESCs showed that miR-320 is independent of DGCR8 and dependent on Dicer. This results lead to the model that RNA polymerase III transcribes short hairpins that are directly processed by Dicer, without a requirement for Drosha. The exact

mechanism for pre-miR-320 processing and its biological role is not defined (Babiarz et al., 2008).

In flies and nematodes Dicer-2 cleaves long dsRNA as part of the viral immune response (Li et al., 2002; Sarkies et al., 2013). Endogenous long dsRNA transcript from transposons and cis-natural antisense transcript only processed by Dicer and give rise to endogenous short interference RNAs (endo-siRNAs) (Watanabe et al., 2008). In vertebrates endo-siRNAs are reported in embryonic stem cells (ECS) and oocyte (Babiarz et al., 2008; Watanabe et al., 2008). Antisense transcribed pseudo genes form long dsRNA. They enter the small RNA pathway by Dicer cleavage and produce endo-siRNAs (Tam et al., 2008).

A Drosha-dependent and Dicer-independent miRNA, miR-451, is conserved in vertebrates (Yang et al., 2010). The Drosha product is only ~36 nucleotides long and too short for Dicer processing. The short pre-miRNA is exported to the cytoplasm, where it directly binds to Argonaute proteins. In mammals only pre-miR-451 loaded into Argonaute 2 matures further, because the slicing activity, which is essential for miR-451 maturation, is lost in Argonaute 1, 3, and 4 (Meister, 2013). Argonaute 2 slices the 3' arm of pre-miR-451 and the remaining ~30 nucleotide 5' arm is shorten by an unknown nuclease (Cifuentes et al., 2010) (Cheloufi et al., 2010).

In summary the origin of mature miRNAs is very diverse. Many molecules that mimic a canonical substrate for the enzymes of the miRNA biogenesis machinery can be a potential small RNA with silencing function. Good evidence lacks for the biological function of many of these small RNAs. In many cases, low-abundant Argonaute-bound small RNAs may reflect occasional and perhaps accidental assembly of RNA decay intermediates into RISC.

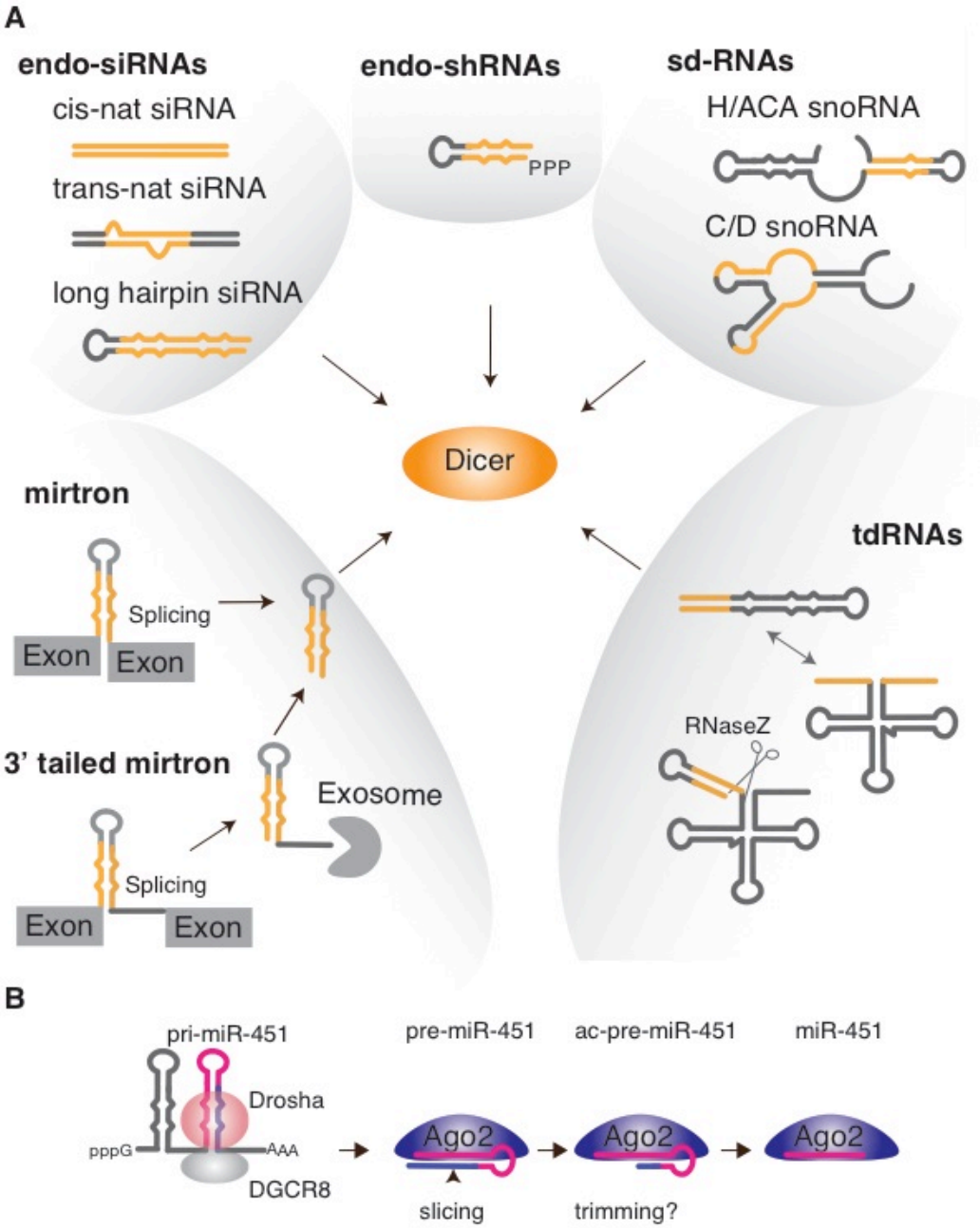


**Figure 1.2 The diversity of non-canonical miRNA** (A) Drosha independent/Dicer dependent small RNAs have a very different origin. Endogenous long dsRNA transcripts from transposons, cis-natural antisense transcript or long hairpins give rise to endogenous short interference RNAs. RNA Polymerase III transcribes endo-short hairpin RNAs. Small nucleolar RNAs derive from C/D box- and H/ACA-snoRNAs. Short introns give rise to small RNAs. The splicing machinery determines both ends of the mirtrons. For 3' tailed mitrons one end is defined by the splicing event and the other by the Exosome. tRNA derived small RNAs (tdRNAs) derive from RNaseZ cleaved 3' tails of tRNAs. Alternative folding of tRNA-Ile into a long hairpin that is processed by Dicer can create tdRNAs. (B) One Drosha dependent/Dicer independent miRNA is known. Drosha cleaves the primary-miR-451 into a short hairpin that is directly loaded into the Argonaute 2 protein. Argonaute 2 itself slices one strand and a unknown slicing event generates the mature miR-451.

### Mechanisms of small RNA-mediated gene regulation

A miRNA duplex must be loaded into an Argonaute protein to mediate gene regulation. A ~22 nt single stranded small RNA remains in the Argonaute protein (guide strand) and together they from the active RNA-induced silencing complex (RISC) (Kawamata and Tomari, 2010). Argonaute proteins organize the guide strand into domains. Thereby initial binding of miRNAs to the target mRNA occurs via the guide strand seed region (nucleotides 2 to 7 or 8) (Han et al., 2009; MacRae et al., 2008; Wang et al., 2008). The nucleotides 13 to 16 (3′-supplementary sites) can increase binding affinity (Grimson et al., 2007; Yekta et al., 2004). The primary factor in target prediction of miRNAs is conservation in target sequences. miRNAs are predicted to target hundreds of mRNAs with their seed region and each individual mRNA can be targeted by multiple miRNAs (Brennecke et al., 2005; Meister et al., 2004). The precise prediction in silico is very difficult, because many factors influence miRNA:target binding. Beside the already mentioned binding affinity, the context of the target site (Grimson et al., 2007; Yekta et al., 2004) and especially the relative abundance of miRNA and their target mRNAs determines the degree of regulation. Only the most abundance miRNAs are capable of regulating their targets (Mullokandov et al., 2012; Wee et al., 2012). The regulation of genes occurs in a target-specific and post-transcriptionally manner in the cytoplasm. The general mechanisms mediating the regulation are still under discussion. Among the proposed mechanisms are repression of translation initiation and elongation, as well as non-specific mRNA decay (Huntzinger and Izaurralde, 2011). Only a few miRNA:target mRNA pairs exhibit a high enough complementarity that induced Argonaute-directed endonucleolytic mRNA cleavage (Karginov et al., 2010). The majority of miRNAs bind to their target mRNA only via the seed region, however they induce decay of target mRNA abundance (Guo et al., 2010) and cause to a great extend the reduction protein abundance (Baek et al., 2008). Nevertheless the inhibition of translation contributes to gene regulation (Guo et al., 2010;

Mathonnet et al., 2007). In flies the GW182 protein, in mammals three paralogs TNRC 6A, B and C exist, mediates miRNA-mediated translation repression and miRNA-mediated mRNA decay (Eulalio et al., 2009). The N-terminal half of GW182 binds to the Argonaute protein and the C-terminus harbors a silencing domain. It is suggested that for miRNA-mediated regulation the silencing domain binds proteins like PARB that binds other factors involved in mRNA circulation, deadenylation and decay (Fabian and Sonenberg, 2012; Huntzinger and Izaurralde, 2011).

In contrast endo- and exo-siRNAs regulate gene-expression mainly by Argonaute-mediated endonucleolytic mRNA cleavage to defend hosts, such as flies and worms, against transposons and viruses (Golden et al., 2008; Martinez and Tuschl, 2004). They are loaded into the slicer active Argonaute proteins (Meister et al., 2004). Then they bind to a full complementary target mRNA and mediate cleave of the target mRNA by the Argonaute protein (Liu et al., 2004). The Argonaute protein cleaves and creates mRNA fragments with 5' monophosphate and 3' hydroxyl termini (Martinez and Tuschl, 2004). The 5' mRNA fragment is degraded by an exosome-mediated decay, whereas the 3' mRNA fragment is degraded by the major cytoplasmic 5'-to-3' exonuclease XRN1 (Orban and Izaurralde, 2005).

### Regulation of miRNA biogenesis and function

The ratio of miRNA to target mRNA is key for the regulatory function (Wee et al., 2012). Changes in miRNA processing and turnover regulate miRNA abundance and thus tune their regulatory effect. The abundance of miRNAs is currently believed to be mainly regulated by transcription factors (Xu et al., 2009). Beyond this, RNA binding proteins and microprocessor modifications alter Drosha processing for specific pri-miRNAs (Guil and Cáceres, 2007; Siomi and Siomi, 2010). Drosha and DGCR8 abundance regulates general miRNA homeostasis. Therefore constant Drosha and DGCR8 levels are important for stable miRNA production (Han et al., 2004; Lee et al., 2003). Drosha negatively regulates

DGCR8 protein levels through cleavage of two hairpins in the *dgcr8* mRNA. DGCR8 protein positively regulates Drosha by protein-protein stabilization. This crossregulation ensures that Drosha and DGCR8 protein levels can be adjusted to microprocessor substrate levels (Han et al., 2009).

Regulation of Dicer processing is best studied for the RNA binding protein Lin-28 and the *let-7*-familiy miRNAs (Heo et al., 2008; Viswanathan et al., 2008). In embryonic stem cells, Lin-28 binds to the loop of *let-7* precursors and blocks *let-7* maturation (Newman et al., 2008). *Let-7* targets are proteins essential for the maintenance of pluripotency and the undifferentiated state. During differentiation Lin-28 expression is lost and pre-*let-7* matures (Viswanathan et al., 2008).

A general regulation of Dicer function is suggested by phosphorylation of TRBP. Loss of the Dicer partner protein TRBP destabilizes Dicer and impairs pre-miRNA processing (Melo et al., 2009). The MAPK signaling pathway phosphorylates and stabilizes TRBP. It is suggested that the increased TRBP abundance can stabilize Dicer and increase miRNA processing (Paroo et al., 2009).

Like TRBP, also Argonaute proteins are post-translationally modified (Meister, 2013). But if and how these modifications regulate miRNA function is less clear. The poly(ADP-ribose) polymerase modifies Argonaute proteins and increases the regulatory ability during stress response (Leung et al., 2011). Lack of Argonaute 2 reduces specific miRNA concentration (Shekar et al., 2011) and post-translational modification with Prolyl 4-hydroxylation stabilizes Argonaute (Qi et al., 2008). Regulation of Argonaute protein could regulate miRNA abundance and their regulatory potential.

Other mechanisms for regulation of processing and turnover are reported (Siomi and Siomi, 2010). They suggest regulation on all levels of miRNA pathway via accessory proteins and protein and RNA modification, but their overall contribution to miRNA function is unclear.

### Application of small RNAs

The application of small RNAs as gene regulatory agents became a powerful tool in experimental science to discover gene functions in cultured cells and in vivo (Elbashir et al., 2001; Kennerdell and Carthew, 1998; Timmons et al., 2001). Exogenously supplied RNA hijacks the endogenous RNA interference pathway and down-regulate the protein coding genes of choice (Elbashir et al., 2001). Due to the simplicity of the technique, high-throughput genome wide genetic screens in multiploid systems became feasible and successfully contribute to elucidate the role of small RNAs in many biological processes like cell cycle, apoptosis and signaling (Bosher and Labouesse, 2000). The therapeutic potential of RNAi is currently tested in clinical trails to target a range of diseases from dermal scarring, viral infection to cancer (Haussecker, 2012). The safety, mechanism of action and clinical activity of RNAi therapeutics could been shown in humans and have proven the concept of RNAi therapeutics (Tabernero et al., 2013). Since pharmaceutical RNAi and endogenous miRNAs mediate their function by the same pathway in mammals, the further understanding of the miRNA pathway and mechanism is crucial for the application of RNAi therapeutics.

## 1.2 Forward genetic screens

Forward genetic screens identify genes associated with a specific phenotype. A starting population is genetically modified and selected for a specific phenotype. After identification of the mutated genes, the gene function can be studied in more detail (Grimm, 2004). Genetic screens in worms and flies helped to discover many factors of the miRNA pathway (Lee et al., 2004b; Tabara et al., 1999). But in mammals genetic screens are technically challenging. The most suitable organism is mouse, however a genome wide genetic screen in mice is time and cost intensive (Kile and Hilton, 2005). A much less cost and labor-intensive system is tissue culture. On the other hand the *ex vivo* system has two

major problems that rise from the inability of crossing and inbreeding, discussed in the following paragraph (Grimm, 2004).

In all organisms the genome contains all the hereditary information. In eukaryotes the entire information organizes in a set of chromosomes. Chromosomes consist of the information for RNA and proteins. Every mammalian cell, except the gametes, contains two sets of chromosomes and thereby twice the entire information. This status is called diploid, a favorable characteristic in evolution, because a second copy of gene can compensate for loss of function in the other gene (McKusick and Chase, 1973). For a forward genetic screen, this implies that for many genes only the perturbation of both copies generates a phenotype. The chances to generate a mutant phenotype are very low, because the mutagenesis needs to perturb both alleles of a gene. Another problem are multiple mutated genes in one cell. In this case, the clear association of phenotype to one gene is impossible. In animals inbreeding and crossing handle the gene compensation by the second allele and multiple mutated genes. Homozygous alleles are generated and excessive mutations are removed. However recent development of retroviral mutagenesis and haploid mouse embryonic stem cells overcome the two major problems in forward genetic screens in mammalian tissue culture (Leeb and Wutz, 2011; Schnütgen et al., 2008).

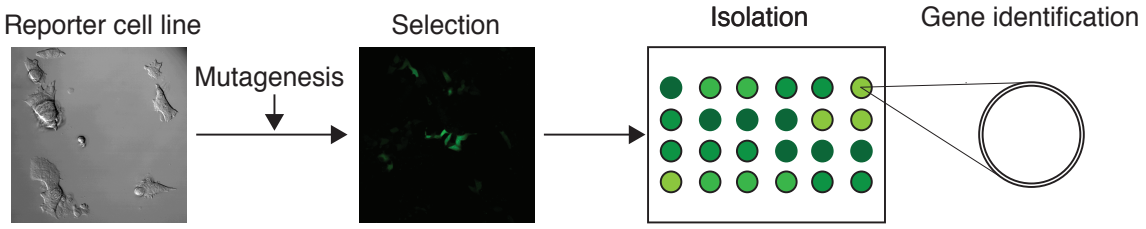


**Figure 1.3 Workflow for forward genetic screens** A starting population of a model organism of choice is genetically modified and selected for a specific phenotype. Single mutated model organisms are isolated and mutated gene genes are identified.

**Mouse embryonic stem cells**

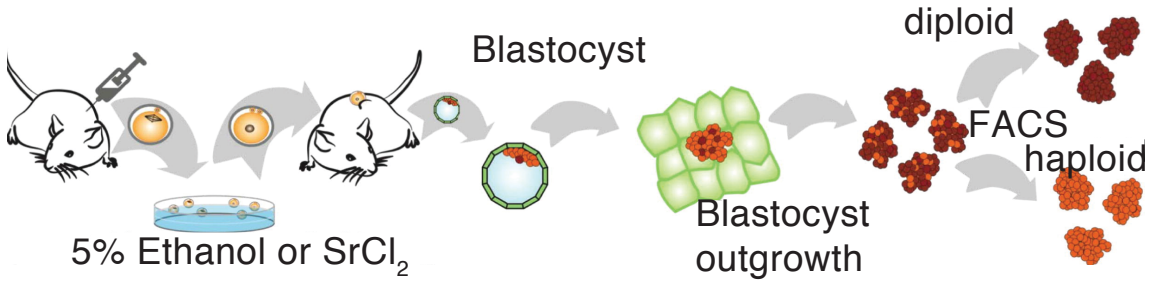


**Figure 1.4 Generation of haploid mouse embryonic stem cells (mESCs)** An oocyte is activated with Ethanol or strontium chloride, mimicking fertilization. The oocyte is transplanted in a pseudopregnant mouse and grows to a blastocyst. The grown blastocyst is transferred into tissue culture and by fluorescence activated cell sorting a small fraction of haploid cells is obtained. **(Elling et al., 2011)**

The first mouse embryonic stem cells were isolated from the inner cell mass of a developing mouse embryo in 1981. They can differentiate to embryoid bodies, a structure harboring all three-germ lineages – endoderm, ectoderm, and mesoderm. mESC introduced into a blastocyst give rise to chimeric mice (Nagy et al., 1990). In cell culture they divide indefinitely and stay undifferentiated. They express Oct4, Sox2 and Nanog, core transcriptions factors of stem-cell renewal (Navarro et al., 2012). Four miRNA clusters generate the most abundant mature miRNAs. The seed region of these miRNAs are highly similar and are associated to the regulation of maintenance and establishment of pluripotency (Kaspi et al., 2013). Haploid mouse embryonic stem cells do not differ in their physiology or molecular profile. The generation of haploid mESCs begins with the artificial activated oocyte. The dividing oocyte grows to a blastocyst and by fluorescence activated cell sorting for low DNA content a small fraction of haploid cells is obtained. Haploid mESC are the ideal model system to avoid heterozygous alleles during mutagenesis thus allow a higher mutagenesis efficiency (Leeb and Wutz, 2011).

**Gene manipulation in mammalian forward genetic screens.**

In a forward genetic screen the model organism is manipulated to generate a desired phenotype. Manipulation strategies should alter the gene expression

efficiently and cover the entire genome (Friedman and Perrimon, 2004). RNAi became a powerful tool due to the specificity reduction of gene products, low cost and high-throughput compatibility (Boutros et al., 2004; Echeverri and Perrimon, 2006). The specificity of RNAi allows correlating a phenotype to one gene and renders crossing and inbreeding unnecessary (Friedman and Perrimon, 2004). On the other hand RNAi is limited to the transient generation of a hypomorphic state and is suboptimal to study the small RNA pathway, because of the interdependency of RNAi function and the studied mechanism. A permanent perturbation of gene function facilitates the phenotype identification and the following analysis. Retroviral constructs efficiently integrate transgenes into the genome (Schnütgen et al., 2005). So called retroviral gene-trap vectors integrate transcription-terminating sequences into the genome and can cause a permanent alteration of the gene function (Hansen et al., 2008). Two major advantages of retroviral mutagenesis are the simple identification of the perturbed gene by inverse PCR and deep sequencing and efficient mutant recovery. The integration of known sequences facilitates mutated gene identification and precise control of transduction efficiency generates mostly mutated model systems with one altered gene per genome.

## 1.3 Project Outline

Much of what is know about the small RNA pathway in mammals is inferred from genetic screens performed in worms and flies. The recent development of haploid mESCs and gene-trap-based mutagenesis enable us to directly address the genetic requirements for murine small RNA pathways.

As a proof-of-principle for such a screen, we wanted to understand if enhanced gene-trap mutagenesis generates core mutants of the small RNA pathway that can be recovered from a screen. Therefore we characterize a mESC lines bearing an enhanced gene-trap insertion in the *Drosha* gene, fortuitously isolated from random mutagenesis of haploid mESC. Furthermore, for a selective screen we tested reporter constructs that should enable the robust and efficient

uncovering of components of murine small RNA silencing pathways. After the validation of the mutagenesis approach and reporter construct in mESCs, we aim to perform a screen in order to identify novel components of the small RNA silencing pathway and generate a rich source of mutant alleles in mammalian small RNA pathway factors.

# 2 Results

## 2.1 Characterization of *Drosha* mutant mESCs

### Description of the *Drosha* mutant locus

Retroviral mutagenesis improved the manipulation and subsequent identification of genes in forward genetic screens. In mESCs, a mutagenesis method called enhanced gene-trap was used for insertional gene manipulation (De-Zolt et al., 2009). The technique combines gene disruption, report for genome integration and detection of low expressed genes in one retro-viral construct: An osteopontin enhancer element increases transcription at the integrated locus. A β-galactosidase/neomycinposphotransferase cassette reports the integration. A splicing acceptor site disrupts gene function, because the newly introduced splicing acceptor site triggers a splicing event that generates a fusion protein of the truncated gene product and β-galactosidase-/neomycinposphotransferase. Finally, a premature polyadenylation signal initiates 3′-end-processing and poly adenylation of the transcript (Schnütgen et al., 2008). The enhanced gene-trap integrates randomly into the genome in sense or antisense direction (Schnütgen et al., 2008), but only sense integrations into transcription units inhibit gene function. Cre recombinase recognition (loxP) sites and flippase recognition targets (FRT) flanking the gene-disruption casette allow to revert the orientation after transient expression of Cre recombinase (Cre) and flippase (Figure 2.1) (Kühn and Torres, 2002; O'Gorman et al., 1991).

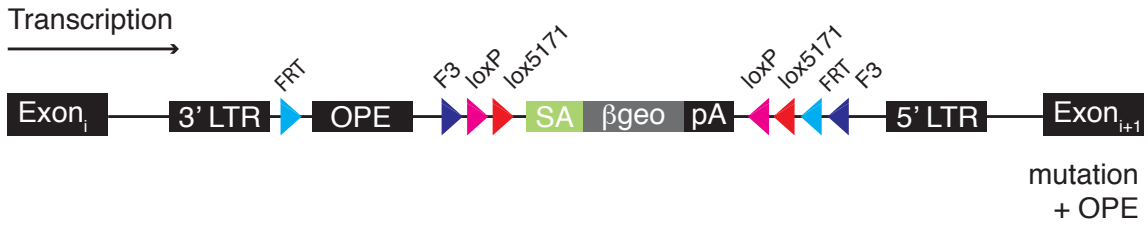


**Figure 2.1 Schematic of enhanced gene-trap in sense orientation.** Long terminal repeats (LTR) flank the osteopontin enhancer element (OPE) and the gene-trap (Splicing acceptor site (SA), β-galactosidase-/neomycinposphotransferase (βgeo) and polyadenylation signal (pA)). The sense integration manipulates the gene function. Expression of Cre recombinase and Filpase allows the excision of the OPE sequence and to revert the orientation of the gene-trap.

In the past, two conditional *Drosha* mutant mice were generated. One was generated using conditional knock-out deletion of exon nine causing multiple premature stop condons in exon eleven (Chong et al., 2008). The other harbors an enhanced gene-trap-like gene inactivation cassette (GIC) in intron four (Teta et al., 2012; Xin et al., 2005). In both cases, similar phenotypes in growth, size and integument were observed, which were generally less severe for the GIC *Drosha* mutant mice (Teta et al., 2012). *Drosha* knock-out mice die after before embryonic day E10.5 (Chong et al., 2008). The International Mouse Strain Resource (Eppig and Strivens, 1999; Kile and Hilton, 2005) reports more the 40 different mESC lines harboring gene-trap insertion in one allele of the *Drosha* gene generated in large scale insertional mutagenesis projects (Hansen et al., 2003; Stryke et al., 2003). But none of these was analyzed in detail. Recently, a haploid mESC line was generated by antisense insertion of the enhanced gene-trap into the *Drosha* locus (Elling et al., 2011). Transient expression of Cre orientated the enhanced gene-trap in the active sense direction and generated the *Drosha* mutant mESC line. The enhanced gene-trap is integrated in the 23$^{rd}$ intron of *Drosha* resulting in a truncated mRNA. The dsRBD at the C-terminus should be lost, as well as the function of the two RNAseIII domains (Figure 2.2).

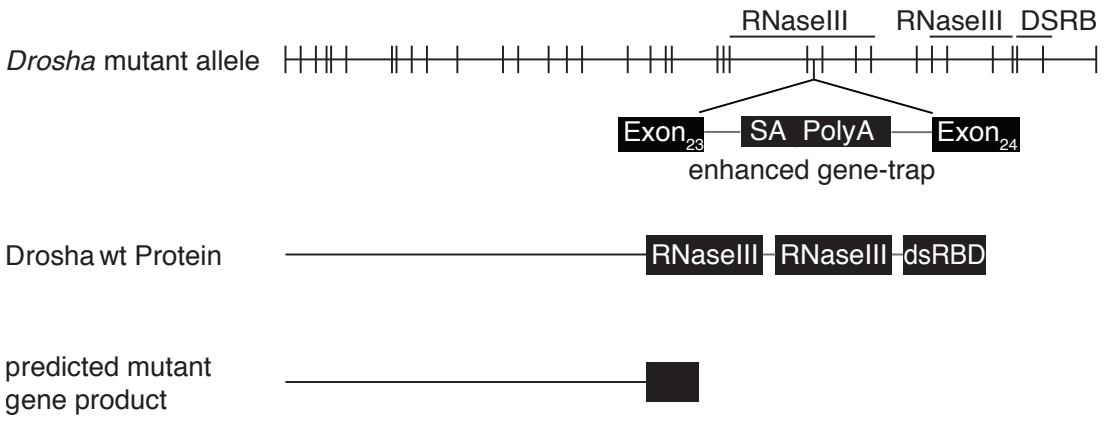


**Figure 2.2 Schematic overview of the mutant *Drosha* allele and its gene products.** The enhanced gene-trap was integrated in the 23rd intron. The predicted mutant gene product lost the dsRBD and both RNaseIII domains.

A retinoic acid-induced differentiation assays showed that the sense-orientated enhanced gene-trap in *Drosha* mutant mESCs leads to a defect in into cystic embryoid body formation (Elling et al., 2011). Furthermore, *Drosha* mutant mESCs fail to repress a reporter transcript upon expression of a potent miR-30-based shRNA (Elling et al., 2011). Both phenotypes are consistent with a defect in the miRNA pathway. When oriented in antisense, the enhanced gene-trap insertion did not produce any noticeable phenotype.

### Gene-trap mutagenesis generates a core miRNA pathway mutant

We initially set out to verify that enhanced gene-trap mutagenesis at the *Drosha* locus generates a mutant phenotype for a core miRNA pathway member. First we confirmed that the gene-trap reduces the abundance of *Drosha* gene products. When analyzed by reverse transcription and quantitative polymerase chain reaction (RT-qPCR), *Drosha* mutant mESCs express approximately 100-fold less *drosha* mRNA compared to the mESC containing the enhanced gene-trap insertion in antisense orientation (hereafter referred to as *Drosha* wt mESCs) (Figure 2.3). In Western blot analysis we were unable to detect Drosha protein in lysate derived from *Drosha* mutant mESCs. A titration of *Drosha* wt mESC lysate, revealed that a dilution of 1/16 fails to generate a detectable signal for Drosha, suggesting that *Drosha*-mutant mESC lysate contained at least 16-fold less

Drosha protein compared to *Drosha* wt mESCs (Supplementary Figure 2). In summary we concluded that the insertion of an enhanced gene trap results in a significant decrease in *Drosha* gene products.

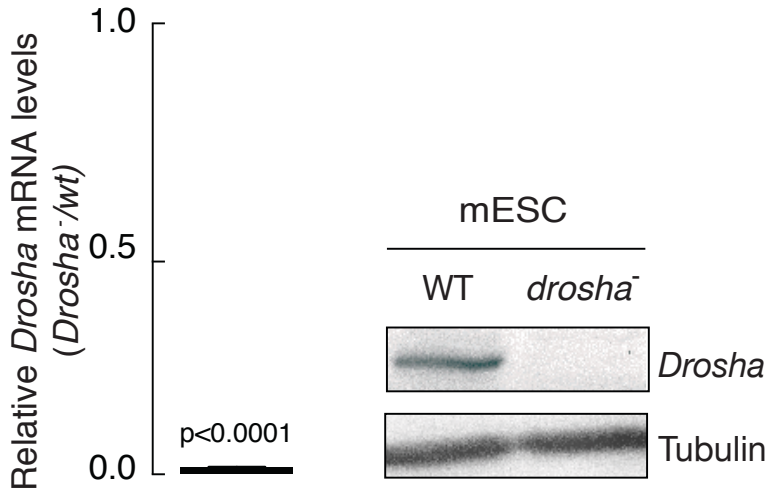


**Figure 2.3 qPCR and Western Blot analysis of *Drosha* gene products.** *Drosha* mRNA and protein are depleted by the enhanced gene-trap insertion. The average and the standard deviation of three biological replicates are depicted in the graph. One tailed student t-test was performed.

Drosha initiates the miRNA pathway by catalyzing the processing of pri-miRNAs to pre-miRNAs in the nucleus. In order to determine the functional consequences of enhanced gene trap insertion at the *Drosha* locus on pri-miRNA levels we performed RT-qPCR analysis of pri-miRNA transcripts. We selected three pre-miRNA transcripts (two polycistronic transcripts and one transcript encoding one miRNA) that all give rise to highly abundant miRNAs in mESCs (Chiang et al., 2010) and designed primer-pairs spanning each miRNA-hairpin as well as regions 5´ and 3´ of the miRNA hairpins (Figure 2.4 A and B).

The miR-290 cluster, encoding the miRNAs miR-290 to miR-295, is the main source for mature miRNAs in mESCs, contributing to more than 45% of all miRNA reads when analyzed by high-throughput sequencing (Kaspi et al., 2013). For the miR-290 cluster, we determined that all seven different miRNA-hairpin spanning amplicons reported at least a three-fold accumulation (fold change = 4.140 ± 0.3086 for miR-290, $p < 0.0032$;

fold change = 4.459 ± 0.4450 for miR-291a, $p < 0.0055$; fold change = 3.250 ± 0.2518 for miR-291b, $p < 0.0041$; fold change = 4.451 ± 0.7477 for miR-292, $p < 0.0153$; fold change = 3.700 ± 0.6054 for miR-293, $p < 0.0164$; fold change = 4.205 ± 0.3785 for miR-294, $p < 0.0046$; fold change = 3.653 ± 0.5578 for miR-295, $p < 0.0144$) The amplicon located at the 3´ end of the miR-290 cluster was similar enriched (fold change = 3.083 ± 0.2515 for 3' of miR 295, $p < 0.0048$). In contrast, the amplicon located 5´ of the miR-290 cluster did not change significantly (fold change = 0.7286 ± 0.08567 for 5' of miR 290, $p < 0.0316$). This discrepancy may be explained by the fact that the ends of the miR-290 cluster are not well defined (NCBI37/mm9) (Meyer et al., 2013), raising the possibility that the 5´ amplicon lies outside the cluster transcript (Figure 2.4 C). The second miRNA cluster we tested contains the miRNAs miR-96, -182 and -183. This transcript accumulates as well in the *Drosha* mutant, but the enrichment is with at least 14 fold higher than the one we found for the miR-290 cluster (fold change = 14.000 ± 0.8906 for miR-182 of, $p < 0.0016$; fold change = 33.350 ± 2.349 for miR-96 of, $p < 0.0018$). This difference may be explained by different transcription rates of the hairpin clusters. Interestingly, the enrichment of the non-hairpin spanning region was less in comparison to the hairpin regions (fold change 3.742 = 0.2256 ± for 3' of miR-182, $p < 0.0022$; fold change 3.758 = 0.6697 ± 3' of miR-96, $p < 0.0191$) (Figure 2.4 C).

Finally, we also observed an increase in the pri-miRNA transcript containing miR-135b (fold change 2.369 = 0.8282 ± for miR-135b, $p < 0.0455$). Like in the case of the miR-290 cluster, the primer set amplifying a fragment located upstream of the hairpin did not show any significant change (fold change 2.129 = 1.278 ± 5' of miR-135b, $p < 0.2657$) (Figure 2.4 C).

In summary, depletion of Drosha results in an accumulation of pri-miRNAs, consistent with a function of Drosha in the processing of these hairpin-containing transcripts.

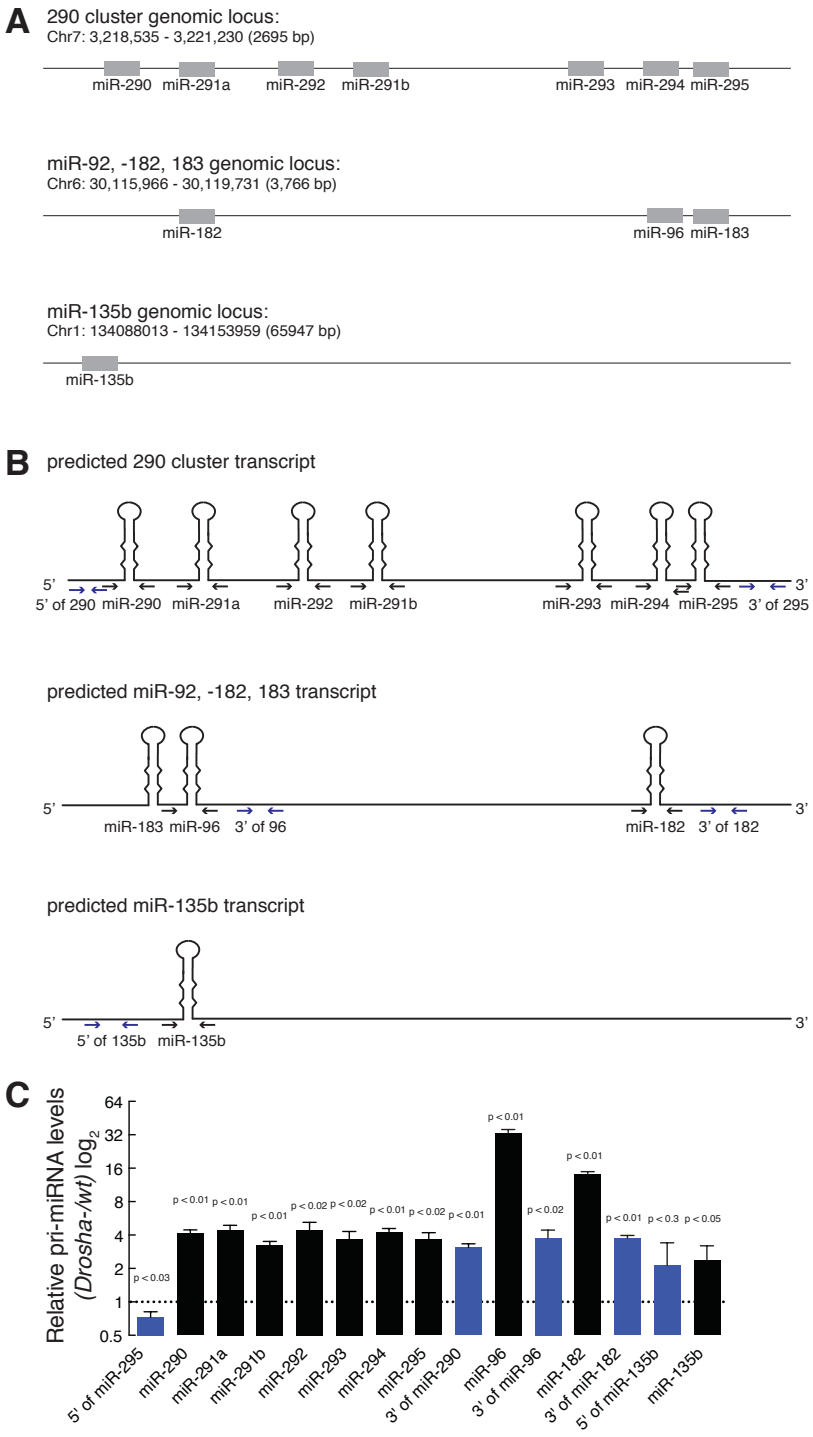


**Figure 2.4 Overview of genomic loci and predicted transcripts of qPCR analysis of primary-miRNAs.** (A) Position and relative distance of miRNA hairpins is indicated for three different genomic loci. (B) Primer position for quantitative analysis of pri-miRNA abundance is indicated for sequencing cleaved by Drosha (black) and regions up (5') and downstream (3') of pre-miRNA sequences (blue). (C) Depletion of Drosha leads to insufficient processing of pri-miRNAs. The average and the standard deviation of three biological replicates are depicted in the graph. One tailed student t-test was performed.

To determine the impact of Drosha depletion on the accumulation of mature miRNAs, we performed Northern hybridization experiments with single nucleotide resolution on 13 different miRNAs (Figure 2.5 A). We found that the abundances of all 13 miRNAs were reduced (average relative miRNA abundance $\bar{x}$ = 26% ± 21% *Drosha* mutant/*Drosha* wt) (Figure 2.5 B). One individual miRNA (miR-136) expressed from a different genomic locus showed a smaller decrease on miRNA abundance ($x_i \geq \bar{x}$ + SD, x = relative miRNA abundance [*Drosha* mutant/*Drosha* wt], i = individual miRNA, $\bar{x}$ = mean of relative miRNA abundance SD = standard deviation of relative miRNA abundance) (Figure 2.5 C).

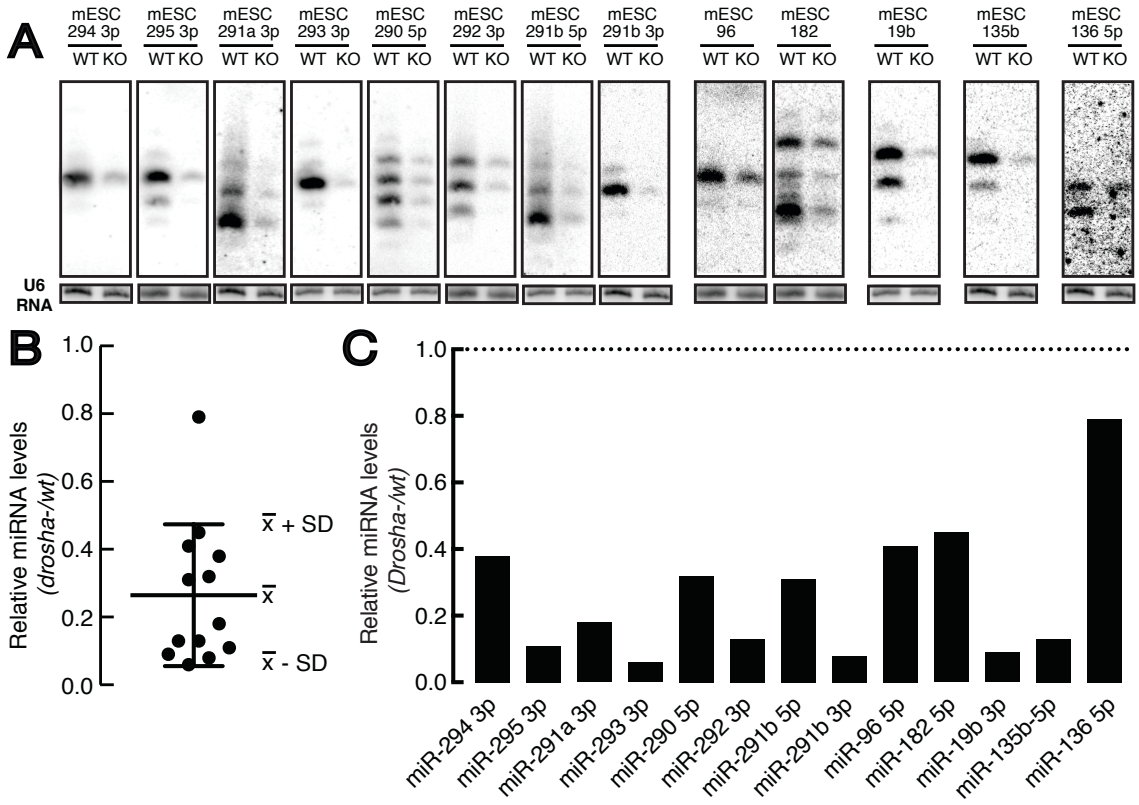


**Figure 2.5 Northern blot analysis for miRNAs.** miRNA abundance is reduced after depletion of *Drosha* gene products. (A) Northern Blot analysis of 13 miRNAs in *Drosha* mutant mESCs. (B) Distribution of 13 analyzed miRNAs. Mean reduction and standard deviation of miRNA levels in *Drosha mutant* ($\bar{x}_I$ = 0.26, SD = 0.14). (C) Quantification of analyzed miRNAs.

For all miRNAs analyzed in Northern hybridization experiments, the isoform distribution did not change (Figure 2.5 A), arguing that perhaps residual Drosha protein levels, undetectable in Western blot analysis, may be present in *Drosha*

mutant mESCs. Therefore, the integration of an enhanced gene trap in *Drosha* mutant mESCs may represent a hypomorphic allele.

We were interested how the entire miRNA population in mESCs changes upon genetic depletion of Drosha. To this end we analyzed small RNA deep sequencing data generated from *Drosha* mutant and *Drosha* wt mESCs by the Brennecke laboratory. Upon mapping to the mouse genome, small RNA reads were classified into non-coding (nc)RNAs (including tRNAs, rRNAs etc.), miRNAs and other RNAs (reads mapping to regions outside of ncRNAs). In the *Drosha* wt mESC library the fraction of miRNA reads (66 %) were more then 3.5 fold higher than in *Drosha* mutant mESCs library (17,7 %) (Figure 2.6 A). In exchange the non-coding RNA and other RNAs fractions in *Drosha* mutant mESCs were around two fold higher. The comparison of the small RNA library requires normalization. In absence of an internal unchanged small RNA fraction miRNAs were normalized to the sum of miRNA and other RNAs reads. The normalization method generates biases when sum and relative relation of the miRNAs and other RNAs differ in-between the two samples. The relative relation is different as wells as the sum. The sum is 55 % in *Drosha* mutant mESCs and 81,4 % in *Drosha* wt mESCs. The deep sequencing analysis indicates an average reduction of miRNA to $\bar{x}$ = 0.46 in *Drosha* mutant mESCs (n = 140) (Figure 2.6 A). Whereas the Northern Blot analysis estimated a stronger depletion of miRNA to $\bar{x}$ = 0.26 in *Drosha* mutant mESCs (n = 13) (Figure 2.5 B). The deep sequencing analysis estimated an average change of $\bar{x}$ = 0.51 fold change for the miRNAs analyzed in Northern Blot. Knowing about the normalization bias, we wanted to correct the overestimation of all small RNA reads in *Drosha* mutant mESCs. Therefore we used the quantification of the Northern Blot analysis. Here, the miRNA quantity can be normalized to an internal independent RNA (U6 spliceosomal RNA [U6 snRNP]).

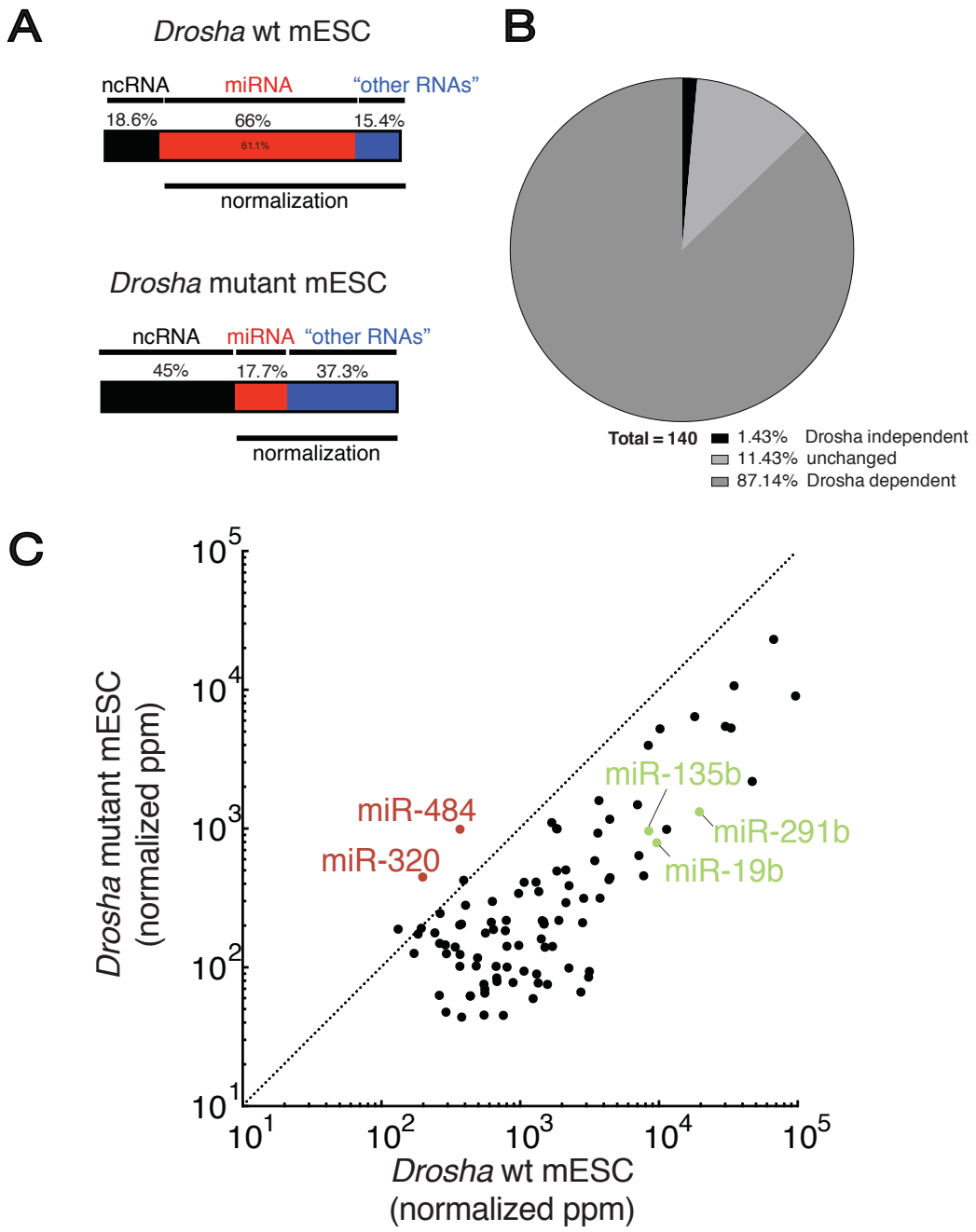


**Figure 2.6 Small RNA deep sequencing analysis of *Drosha* mutant mESCs** (A) Distribution of reads in deep sequencing analysis revealed a smaller fraction of normalizing miRNAs and other RNAs in *Drosha* mutant mESCs compared with *Drosha* wt mESCs. (B) Grouping of miRNAs in *Drosha* dependent, independent and unchanged miRNAs. *Drosha* dependent are at least two-fold depleted in *Drosha* mutant mESCs. *Drosha* independent miRNAs are at least two fold enriched. For unchanged miRNAs no enrichment or depletion of 2 fold was observed. (C) Comparison of miR abundance in *Drosha* wt and mutant mESCs. The deep sequencing reads were normalized to observed changes in Northern Blot analysis. Drosha independent miRNAs are red. miRNAs in green have complementary sites in the endogenous miRNA construct.

Using this approach, we calculated an average two-fold overestimation for each miRNA in deep sequencing (overestimation = 1.96 = 0.51/0.26). Therefore all reads in *Drosha* mutant mESCs were corrected by a factor of 0.5 to normalize the relative miRNA abundance to the observed changes in northern blot analysis.

Of a total of 140 miRNAs, 30% of all miRNAs detected in *Drosha* wt mESCs are not detectable in *Drosha* mutant mESCs. 86% of all miRNAs are at least two-fold downregulated; 11% of all miRNAs are unchanged and only two of 140 analyzed miRNAs (miR-320, miR-484) are more than two-fold upregulated (Figure 2.6 B). Both were previously shown to be DGCR8-independent (Babiarz et al., 2008) (Figure 2.6 C). In *Drosha* mutant mESCs 45% of the miRNAs are derived from the miR-290 cluster. The levels of mature miRNAs of the miR-290-cluster are throughout reduced in *Drosha* mutant mESCs. Outside the 290 cluster, miR-19b and miR-135b are the two most abundant miRNA that are downregulated in *Drosha* mutant mESCs. The two most abundant miRNAs that showed no change upon Drosha depletion are miR-96 and miRNA 182 (Figure 2.6 C).

### ***Drosha's*** **regulatory function in the miRNA pathway**

Drosha and DGCR8 protein are part of the microprocessor and essential for miRNA processing. Furthermore, Drosha and DGCR8 regulate each other post-transcriptionally (Han et al., 2009). Drosha together with DGCR8 cleaves a hairpin-structure embedded in the *dgcr8* mRNA, thereby destabilizing the *dgcr8* mRNA; and DGCR8 stabilizes Drosha protein via complex formation. To test if this cross-regulation is recapitulated in *Drosha* mutant mESCs *DGCR8* gene products were analyzed by RT-qPCR and quantitative Western Blot analysis. As expected *dgcr8* mRNA was increased 5-fold in comparison to *Drosha* wt mESCs (Figure 2.7 A). However, DGCR8 protein levels were not significantly changed (Figure 2.7 B). In contrast, *Drosha* knockdown experiments in human cell culture showed a 3.5 fold increase in DGCR8 abundance (Han et al., 2009). We were interested if depletion of Drosha affects the abundance of other members of the miRNA pathway. For example, published data suggests that Argonaute 2 protein

(Ago2) abundance is reduced if miRNA abundance is decreased (Martinez and Gregory, 2013). In agreement with this finding and along with the fact that depletion of Drosha results in a general decrease in miRNA abundance (Figure 2.6 C), quantitative Western blot analysis revealed a 50 % decrease in Ago2 protein levels in *Drosha* mutant mESCs when compared to *Drosha* wt mESCs (Figure 2.7 B). Interestingly, RT-qPCR analysis of *Ago 2* mRNA revealed a two-fold upregulation in comparison to *Drosha* wt mESCs, suggesting that Ago2 is posttranscriptionally regulated in a Drosha-dependent manner (Figure 2.7 A). The mRNA levels of *argonaute 1*, *trbp*, *pact*, *srp20* and *dicer* were not significantly changed (Figure 2.7 A). Interestingly, the protein levels of Dicer were reduced to 50% in *Drosha* mutant mESCs ($p < 0.01$) (Figure 2.7 B).

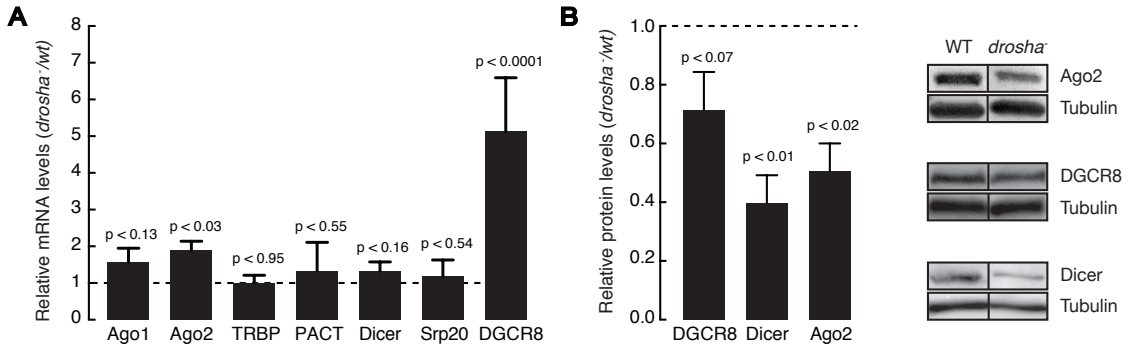


**Figure 2.7 qPCR and Western Blot analysis of components of the miRNA pathway.** (A) *Drosha* mutation deregulates mRNA abundance of *DGCR8* and recapitulates a known cross-regulation of Drosha and DGCR8. (B) Protein abundance of DGCR8 is unchanged, whereas Dicer and Ago2 protein is depleted.

## 2.2 Design of a reporter-based screen to identify the genetic requirements for small RNA-mediated gene regulation in mESCs

Having established that enhanced gene trap-mediated mutagenesis of a core miRNA pathway factor – Drosha – can uncover important features of small RNA-mediated gene silencing, as well as crossregulatory feed-back loops, we aimed to design a reporter strategy in order to determine the genetic requirements for the miRNA pathway in mESCs by a genetic screen. To this end we designed

retro-viral constructs that allow us to monitor perturbations in small RNA-mediated gene regulation based to the derepression of a fluorescence and/or resistance marker, which under normal conditions is repressed by miRNAs. Upon random mutagenesis, any mutation in a gene required for efficient miRNA-mediated gene silencing would result in a stabilization of the marker transcript and an increase in marker translation, which would enable us to identify mutant cell populations by FACS and/or growth under selection conditions.

**Reporter construct responding to endogenous miRNAs**

We initially designed a reporter construct responding to miRNAs endogenously expressed in mESCs. This endogenous miRNA reporter construct consists of two constitutive promoters. The EF1a promoter drives the expression of a control fluorophore (mCherry) to report for successful integration and transcription at the locus of integration. The second promoter (PGK) drives the expression of the reporter fluorophore (Venus) and resistance (Puromycin$^{R}$). A p2a site separates the two genes. The p2a sequence codes for a self-cleaving amino acid sequence and upon translation generates two independent proteins encoded by one mRNA transcript (Kim et al., 2011). The 3´ UTR of this transcript contains five binding sites, perfectly complementary to the miRNAs miR-135b (2 sites), miR-19b (2 sites) and miR-291b (1 site). All three miRNAs are abundantly expressed in mESCs (Figure 2.6 C)

To determine if this construct robustly reports miRNA activity we transduced *Drosha* wt and *Drosha* mutant mESCs with the endogenous miRNA reporter construct. Only successfully transduced cells (mCherry positive) were analyzed in flow cytometry (Figure 2.8 B). In *Drosha* mutant mESCs the mean reporter fluorophore (Venus) intensity was only 2.5 fold higher then in *Drosha* wt mESCs (Figure 2.8 C). The transduced *Drosha* mutant and *Drosha* wt mESCs showed a broad overlap of fluorescence intensity, perhaps because reporter expression is dependent on the site of retroviral integration (Figure 2.8 B). The overlap is predicted to complicate the identification of the small RNA pathway mutants in a

selective screen scenario. Since the expression was analyzed for a heterogeneous population, the isolation of single clones and the analysis of their reporter expression profile could identify a clone with a smaller variation and perhaps increase the sensitivity of the screen.

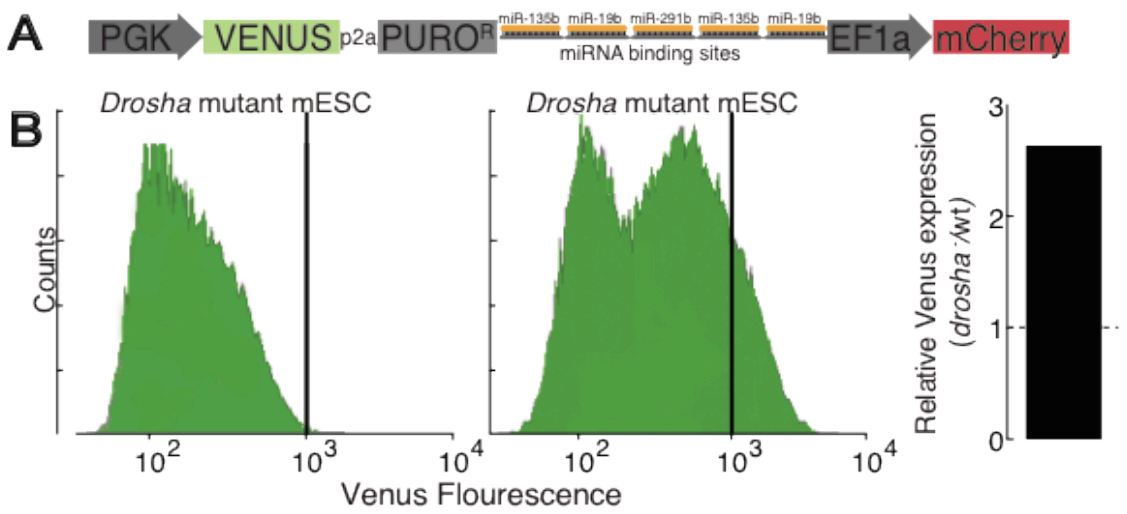


**Figure 2.8 Analysis of reporter sensitivity for perturbed miRNA function. (A)** Schematic of endogenous miRNA reporter. The endogenous miRNA reporter harbors two promoters. The EF1a promoter drives the expression of a control fluorophore mCherry. The PGK promoter drives the expression of a transcript with perfect complement miRNA binding sites for highly abundant endogenous miRNAs in mESCs. Therefore the translation of the protein Venus and Puromycin$^R$ depends on miRNA function. (B) Flow cytometry of transduction of *Drosha* wt and *Drosha* mutant mESCs with endogenous miRNA reporter. Venus fluorescence expression was determined for successful transduced cells (mCherry positive). *Drosha* mutant mESCs showed a 2.5 fold higher Venus expression.

A transient transfection and stable transduction experiment of similar reporter constructs showed deregulation in small RNA pathway mutant. The pSENSOR is a retro-viral construct that consists of a Tet-inducible artificial shRNA and a constitutive promoter driving shRNA regulated Venus fluorescence protein. Mouse embryonic fibroblasts (MEF) transduced with the pSENSOR show a ten-fold suppression of the fluorophore (Fellmann et al., 2011). A transient transfection of a pSENSOR based reporter construct revealed a ten fold derepression in *Drosha* mutant mESCs (Elling et al., 2011). In comparison to the pSENSOR reporter, the endogenous miRNA reporter was less efficiently derepressed in the *Drosha* mutant mESCs (Figure 2.8 C), perhaps because

endogenous miRNA targets compete with the reporter mRNA for miRNA binding and lower the regulatory effect. In contrast the shRNA sequence used in the pSENSOR approach is predicted to only regulate the reporter mRNA. Furthermore, the chosen miRNAs are specifically expressed in mESCs. Spontaneous differentiation upon mutagenesis of mESCs would cause a change in miRNA expression. In summary, we conclude that a reporter regulated by endogenous miRNAs combined with the gene-trap mutagenesis is represents a suboptimal setup for a robust screen in order to identify miRNA pathway components.

### Reporter constructs responding to artificial miRNAs

To increase the reporter sensitivity we designed an shRNA reporter similar to the pSENSOR (Figure 2.10 A). This shRNA reporter consists of two constitutive promoters. The PGK promoter generates the control fluorophore turboGFP (tGFP) (Evdokimov et al., 2006), a fast maturing variant of *Copepods* GFP (Shagin et al., 2004) and a short hairpin harboring a sequence an artificial miRNA, complementary to the coding sequence of *Renilla reniformis* luciferase, placed in the backbone of pre-miR-30 (Dow et al., 2012), modified for efficient Drosha processing (the mature miRNA will be referred to as miR-E). A fraction of tGFP sh-miR-E transcript is expected to be processed by Drosha in the nucleus and generates miR-E. In addition the other fraction of tGFP sh-miR-E transcript is expected to escape Drosha processing and will be translated in the cytoplasm, hence allowing to control of shRNA expression and transduction by monitoring tGFP expression. An EF1a promoter drives the expression of the reporter encoding the fluorophore mCherry-p2a-Puromycin resistance together with four binding sites perfectly complementary to artificial miRNA sequence. As a control, we created one additional control constructs lacking the miR-E hairpin.

To test the new vector design we performed transient transfection experiments in mESCs. In *Drosha* wt and *Drosha* mutant mESCs we observed expression of control fluorophore (tGFP) reporting for the successful transfection, as well the

expression of reporter fluorophore (mCherry) reportings for the response to artificial miRNA regulation. This observation proves the integrity of the shRNA reporter (Figure 2.9). Furthermore we analyzed the response of the reporter construct to the artificial miRNA dependent on the artificial miRNA processing in *Drosha* mutant and wt mESCs. In this non-quantitative experiment the stronger accumulation of yellow signal in the merged picture of the green and red channel indicates the response. As expected the *Drosha* mutant mESCs express more reporter fluorophore in relation to the control fluorophore when compared to *Drosha* wt mESCs, visible by the stronger accumulation of yellow signal in comparison to the *Drosha* wt mESCs (Figure 2.9). This result indicates that the designed construct indeed reports for impaired miRNA-mediated regulation.

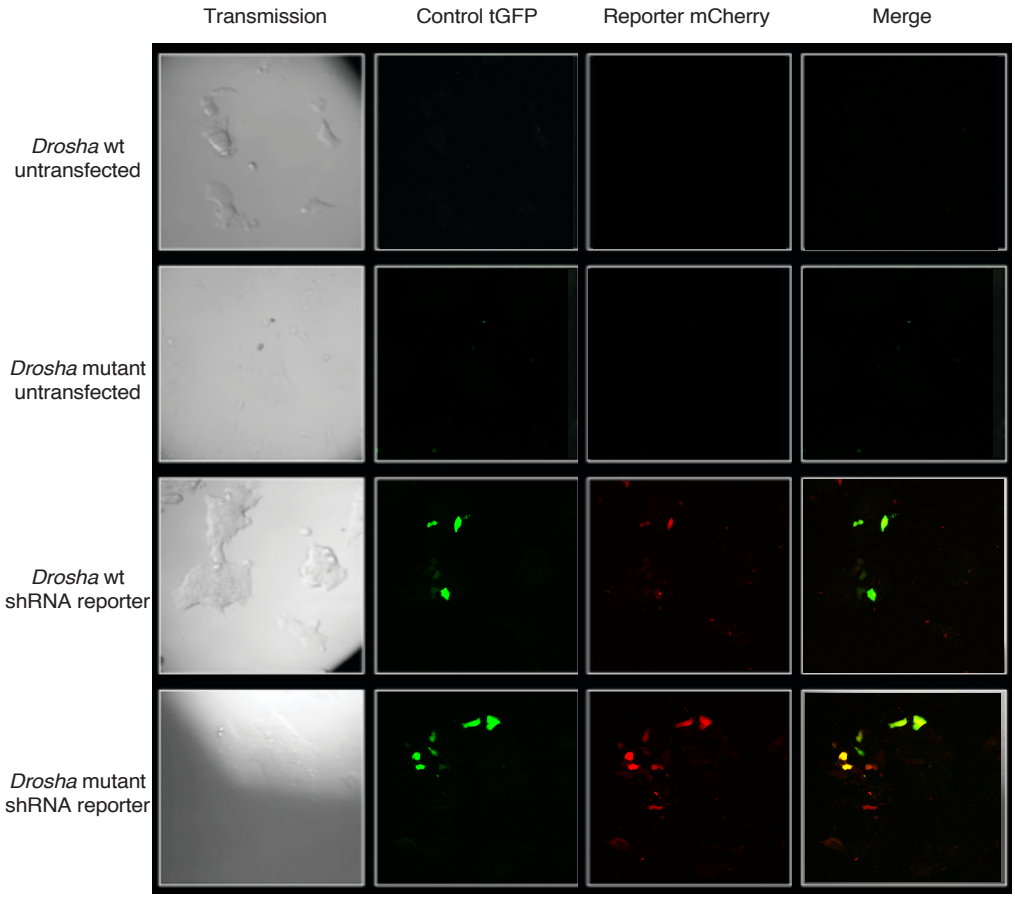


**Figure 2.9 Expression analysis of shRNA-reporter construct**. *Drosha* wt and *Drosha* mutant mESCs were transient transfected with shRNA-reporter construct and fluorophore expression was analyzed by microscopy.

To test the ability to monitor small RNA-mediated gene regulation for the new reporter constructs, *Drosha* wt and *Drosha* mutant mESCs were transduced with the shRNA-expressing reporter and the minus miR-E control construct. (Figure 2.10 B). Control (tGFP) and reporter fluorophore (mCherry) expression detected by flow-cytometry in *Drosha* mutant mESCs was increased compared to *Drosha* wt mESCs, in which expression of both fluorophores was close to the untransfected control (Figure 2.10 B). The two fluorophores of the control reporter construct lacking the miR-E hairpin were expressed to a similar level in *Drosha* wt and *Drosha* mutant mESCs (Figure 2.10 B). In *Drosha* wt mESCs successful transduction is neither reporter confidentially via expression of control nor reporter fluorophore. The differentiation whether a very efficient small RNA mediate gene regulation or inefficient transduction causes the expression of both fluorophores close to the untransfected control is impossible. This uncertainty prevents the comparison of *Drosha* wt and *Drosha* mutant mESCs regarding their small RNA mediated gene regulation. However the successful transduction of the control and report construct in *Drosha* mutant mESCs suggests that *Drosha* wt mESCs were successfully transduced with the reporter construct and the PGK promoter does not generate enough tGFP-miR-E transcripts to translate tGFP protein. Furthermore the same packaged virus was used for transduction of *Drosha* wt and *Drosha* mutant mESCs and a slight shift of the *Drosha* wt mESCs indicates very low transgene expression. Suggesting another possibility for not detectable levels of control and reporter fluorophore: complete conversion of tGFP shRNA transcript by Drosha to shRNA and complete downregulation of the reporter fluorophore. As mention before pSENSOR derived constructs combine the miR-30 backbone with a Tet-inducible promoter to observe small RNA-mediated gene regulation (Elling et al., 2011; Fellmann et al., 2011). Here, the more efficient processed version of the miR-30 backbone, miR-E is coupled with a constitutive PGK promoter.

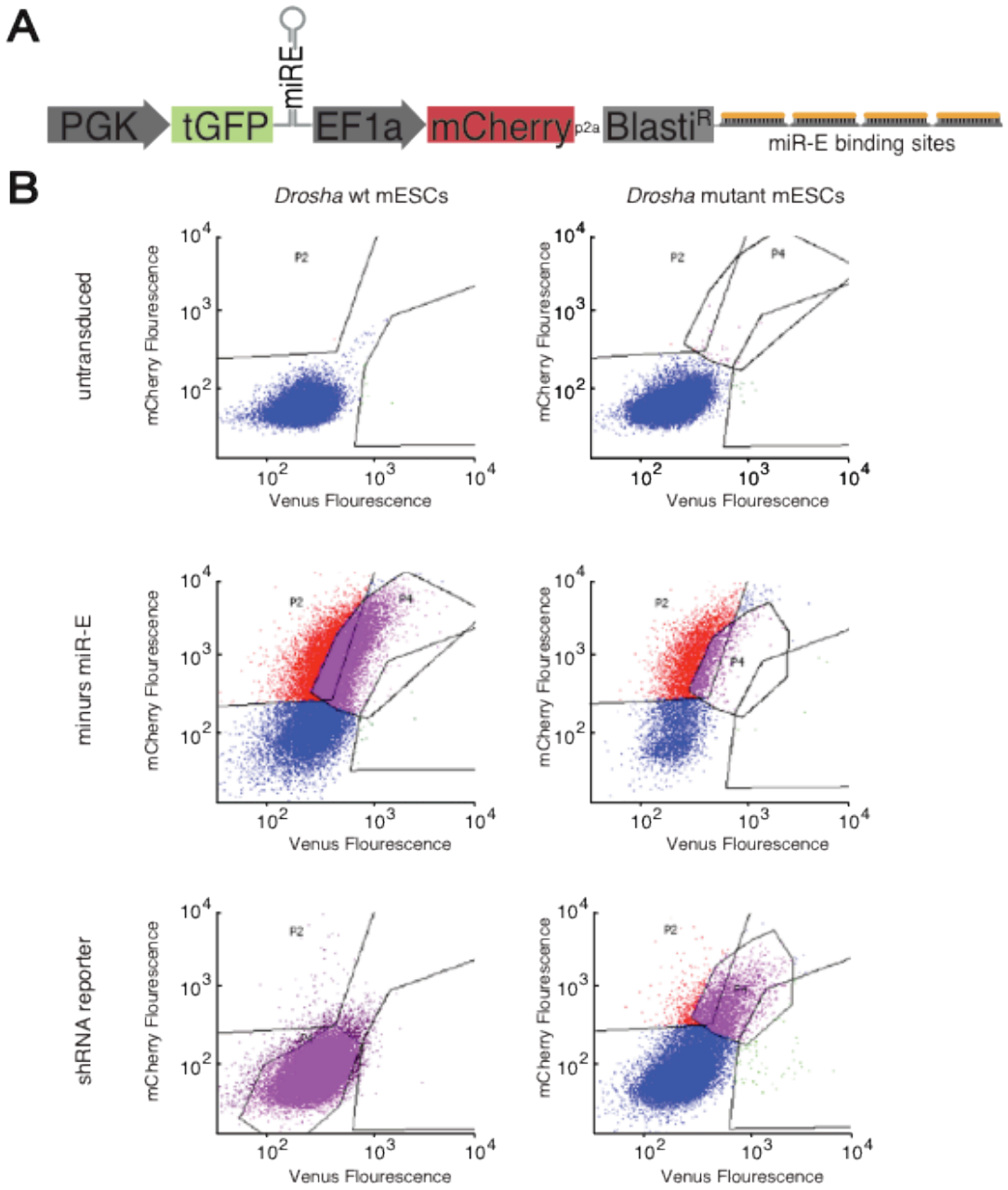


**Figure 2.10 Analysis of sh-RNA reporter sensitivity for perturbed small RNA regulation. (A)** Schematic of sh-RNA reporter construct. The sh-RNA reporter construct harbors two promoters. The PGK promoter drives the expression of a control fluorophore tGFP and the short hairpin miR-E. The PGK promoter drives the expression of a transcript with perfect complement miR-E binding sites. Translation of the protein mCherry and Blasticidin$^R$ depends on small RNA regulation. (B) Flow cytometry of *Drosha* wt and *Drosha* mutant mESCs transduced with sh-RNA reporter and minus sh-RNA control. mCherry and Venus fluorescence expression was determined in flow cytometrie.

The transient transfection in *Drosha* wt mESCs drives enough plasmid transcription to generate both fluorophore (Figure 2.9), perhaps because transcription from multiple plasmids per cell saturates Drosha processing. However transduction of the shRNA reporter integrates only a single copy per cell. The more efficient processing of miR-E and the properly weaker PGK promoter do not saturate Drosha processing and does not allow us to monitor small RNA-mediated gene regulation. Northern Blot for miR-E could support the theory and detected successfully transduced clones. Nevertheless a simple control for transgene transcription is crucial for the selective screen, because retroviral transgene silencing was observed in mESCs (Cherry et al., 2000) and the loss of repression reports for perturbed small RNA pathway.

We want to create a two-step reporter that allows monitoring of small RNA-mediated gene regulation, reporter and control expression. In contrast to the previous constructs the control and reporter fluorophores are separated on two different retro-viral constructs. Sequently integration ensures successful integration of both constructs. An inducible promoter in the second construct allows controlling for expression at any time. Firstly the constitutive expressed reporter genes with exogenous small RNA sites in the 3'UTR are integrated (PGK Venus p2a Puromycin$^{R}$ (miR-EBS)$_4$) (Figure 2.11 A). Single clones are cultured under selection to prevent retroviral transgene silencing (Cherry et al., 2000). Secondly a single clone population is transduced with the artificial miRNA-harboring construct (TRE3G mCherry miR-E EF1α tTA) (Figure 2.11 B). The constitutive EF1α promoter transcribes the tetracycline transactivator (tTA). tTA protein binds to the Tetracycline Response Element 3G (promoter TRE3G) and activates the transcription of mCherry-miR-E. One fraction of the transcript is translated to mCherry protein and the other fraction is Drosha processed and generates miR-E. The TRE3G promoter generated previously miRNA and resistance protein from a Neomycin resistance - miR-30 backbone transcript in mESCs (Fellmann et al., 2011).

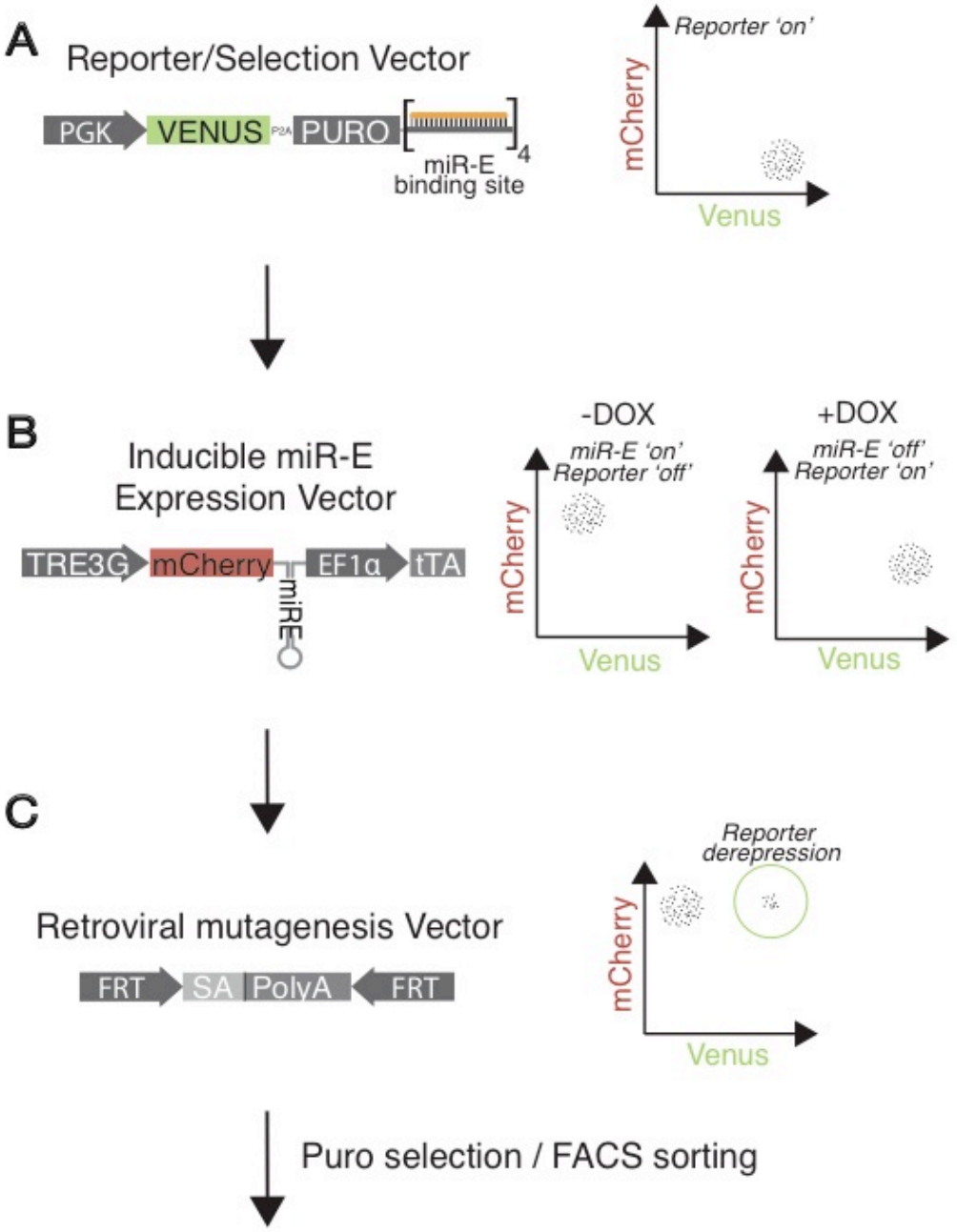


**Figure 2.11 Proposed 2-step reporter cell line generation and mutagenesis approach.** (A) An individual reporter cell line expresses selection markers (Venus and Puromycin$^{R}$) harboring small RNA binding sites in the 3'UTR. (B) The small RNA expression cassette is added and in the absence of doxycycline (DOX) regulation of the selection markers occurs. The addition of DOX blocks the transcription of the regulating small RNA and simulates an impaired small RNA regulation. The selection markers are translated and the regulatory potential of the small RNA is revealed. (C) In the absence of DOX the mutagenesis generates mutants of interest that express the small RNA, but are not able to downregulate the selection markers.

Suggesting that the TRE3G promoter will generate as well mCherry and miR-E. Integration and stable expression of the second construct is reported by mCherry. The generated miR-E represses the reporter transcript.

Nevertheless the expression of the reporter construct can be controlled. Supplied doxycycline, a tetracycline antibiotic, binds tTA and block the transcription of the TRE3G promoter (Figure 2.11 B). The resulting loss of miR-E will release the small RNA-mediated regulation on the reporter transcript and expression can be controlled via detection of (Venus) or selection (Puromycin$^{R}$). The derepression is at the same time the expected window of deregulation in a selective screen setup. For a selective screen a single cell clone has to be isolated and mutagenesis performed. The gain of reporter fluorophore reports for loss of small RNA-mediated regulation (Figure 2.11 C).

# 3 Discussion

Genetic screens in worms and flies helped to elucidate the components of the miRNA pathway (Lee et al., 2004b; Tabara et al., 1999). in a proof-of-principle study, that genetic manipulation via enhanced gene-traps in haploid mESCs enables the identification and characterization of core components of the murine miRNA pathway (Figure 2.3 – Figure 2.7). Thereby we propose that haploid mESCs in combination with enhanced gene-trap mutagenesis may be used in a genetic screen to solve the obstacle of recessive gene compensation, which currently prevents the genetic dissection of small RNA silencing pathway in mammals. Previously, a genetic screen for murine components of the small RNA pathway was performed in diploid mESCs and only recovered mutants in Argonaute 2, a known component of the RISC (Trombly et al., 2009). In that study, the requirements for small RNA pathway were addressed using artificial shRNA regulation on a reporter gene and retroviral mutagenesis (Trombly et al., 2009). A major obstacle of genetic screens in mammals is that recessive gene are compensated by the second allele. The bloom's syndrome protein (*Blm*) contributes to genome stability and in *Blm* mutant mESCs a higher conversion of heterozygous genes to homozygous is observed (Luo et al., 2000; Yusa et al., 2004). In the mentioned screen the *Blm* deficient mESCs inefficiently overcome this difficulty (Trombly et al., 2009). A genetic screen for components of the small RNA pathway in haploid mESCs generates only homozygous mutants and allows us to revisit the genetic requirements for small RNA-mediate gene regulation in mammals.

We established that the enhanced gene-trap mutagenesis generated the first homozygous *Drosha* mutant mESCs with hypomorphic character (Elling et al., 2011). Nonetheless, this cell line recapitulates the molecular and biological function of Drosha and enables the identification of previously described and novel regulatory feedback-loops in the miRNA pathway (Figure 2.3 – Figure 2.7).

Previous studies have also shown that the deletion mutation of two essential components of miRNA biogenesis, DGCR8 and Dicer, leads to a complete loss of canonical miRNAs (Babiarz et al., 2008). *DGCR8* mutant mESCs were generated through the deletion of the 3rd exon, giving rise to a premature stop codon. A strong depletion of canonical miRNAs was observed by microarray analysis and two of the most abundant miRNAs (miR-293 and miR-294) in mESCs were not detectable by Northern Blot analysis (Wang et al., 2007). A similar picture has been shown in *Dicer* mutant mESCs. *Dicer* mutant mESCs were generated through the deletion of the N-terminal located RNAseIII domains (Murchison et al., 2005). The loss of canonical miRNAs is similar to the loss in *DGCR8* mutant mESCs (Calabrese et al., 2007). The insertion of the enhanced gene-trap in to the *Drosha gene,* a core-factor of canonical miRNA biogenesis (Lee et al., 2003), is expected to lead as well to a complete loss of canonical miRNA. But *DGCR8* and *Dicer* mutants mESCs exhibit a profounder depletion of canonical miRNAs levels (Babiarz et al., 2008). The relatively high residual amounts of canonical miRNA in *Drosha* mutant mESCs suggest that the enhanced gene-trap insertion does not completely perturb *Drosha* function (Figure 2.6 C). This is supported by the observation that the phenotype in mice of a gene-trap insertion in the *Drosha* gene causes as well a milder phenotype then deletion of *Drosha* (Chong et al., 2008; Teta et al., 2012). One explanation of the hypomorphic character could be that the gene-trap does not cause 100% efficient mRNA splicing (Sharp et al., 1987). The enhanced gene-trap insertion causes an altered mRNA transcript. The splicing machinery splices at the introduced acceptor site and causes a loss of regular *drosha* transcript. Occasionally the introduced acceptor site could be missed and original *drosha* mRNA would be generated. Another explanation would be an alternative miRNA-processing pathway. The alternative RNAse must be DGCR8 dependent, because in *DGCR8* mutant mESCs canonical miRNA abundance is abolished in spite of unperturbed *Drosha* (Wang et al., 2007).

Only a few regulation mechanism of the miRNA pathway are well understood. One of the best understood mechanism is the crossregulation of *DGCR8* and *Drosha* (Han et al., 2009). In the *Drosha* mutant mESC line we recapitulate the cross regulation of *DGCR8* and *Drosha* (Figure 2.7 and Figure 3.1 A). Furthermore we find that *Drosha* regulates Argonaute 2 and Dicer protein abundance (Figure 2.3 – Figure 2.7): We observed that Drosha abundance impacts Argonaute 2 protein levels (Figure 2.7 B). Previous studies have shown that unloaded Argonaute 2 protein is degraded and that general increased miRNA abundance can stabilize Argonaute 2 protein (Martinez and Gregory, 2013). The decrease in Argonaute 2 protein levels upon Drosha depletion is therefore likely a consequence of the decreased in overall miRNA abundance. We speculate that this type of regulation ensures a rapid removal of empty Argonaute 2 protein in absence of bona-fide miRNAs, which could prevent undesirable loading of Argonaute 2 with aberrant RNA decay intemediates.

Additionally we show that *Argonaute 2* abundance is also regulated at post-transcriptional level (Figure 2.7 A): Upon depletion of *Drosha*, *argonaute 2* mRNA levels increase significantly. While we do not know the underlying mechanism of how Drosha regulates Argonaute 2 mRNA levels one could envision two possible scenarios: (1) Argonaute 2 mRNA contains a relatively long 3' UTR with multiple predicted miRNA binding sites (downregulated in Drosha mutant mESCs compared to Drosha mt mESCs: miR-182, miR-183, miR125a, miR-27a, miR-27b and miR-99; upregulated in *Drosha* mutant mESCs compared to *Drosha* mt mESCs: miR-125b). Therefore Argonaute 2 may be regulated post-transcriptionally regulated by miRNAs, and as a consequence of Drosha-depletion, mRNA levels would increase. (2) As an alternative possibility, Drosha may directly regulate a*rgonaute 2* mRNA levels through a mechanism similar to the one described for *dgcr8* mRNA (Han et al., 2009). However, our superficial mRNA structure analysis failed to detect an obvious hairpin structure that may be targeted by Drosha.

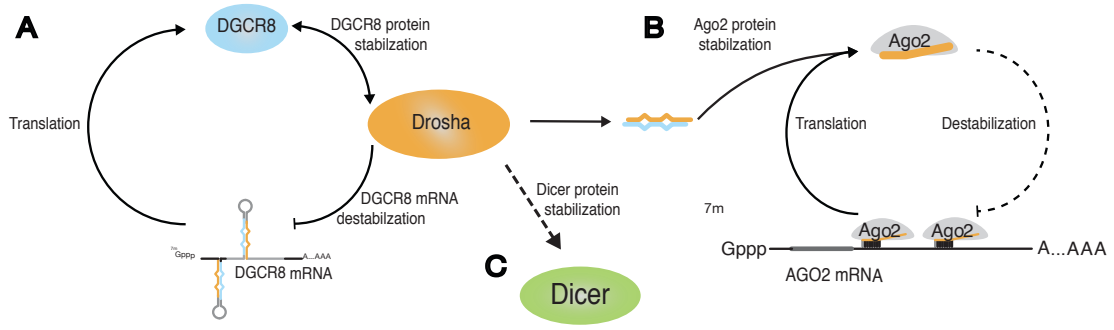


**Figure 3.1 Proposed regulatory function of *Drosha.*** (A) In an autoregualtory feedback-loop *Drosha* and *DGCR8* control their protein abundance. Drosha protein cleaves two hairpins in the d*gcr8* mRNA and destabilizes the transcript. The reduced *dgcr8* translation causes reduction of Drosha protein abundance, because DGCR8 and Drosha stabilize each other via protein-protein interaction. More *dgcr8* mRNA escapes the Drosha processing. The increased translation of DGCR8 protein stabilizes Drosha protein and feedback loop is closed. (B) Furthermore *Drosha* regulates *Argonaute 2* and *Dicer*. We suggest that *Drosha* precede a miRNA-*Argonaute 2* feedback-loop. Newly synthesized miRNAs stabilized Argonaute *2* protein and protect it for degradation. The loaded miRNAs potentially target the long long 3' UTR of *argonaute 2* mRNA. The regulation of *Argonaute 2* mRNA translation guaranties the homeostasis of Argonaute *2 protein*. (C) In addition mutation of *Drosha* affects Dicer protein abundance.

We also show that Drosha stabilizes Dicer at the protein level (Figure 2.7 B and Figure 3.1 C). Upon depletion Drosha, Dicer protein abundance decreases more than 2-fold. The mechanism behind the regulation is unclear. One could envision that Dicer protein stability could be coupled to substrate abundance, which is decreased in the absence of Drosha. In this case one would predict that depletion of other core factors, required for pre-miRNA biogenesis would lead to a similar phenotype. This hypothesis could be tested in *DGCR8* deficient mESCs.

To further dissect the small RNA silencing pathway the goal is to perform a reporter based genetic screen. Here we provide a systematic view on the suitability of different reporter designs that respond to endogenous or artificial miRNAs in order to implement such a screen (Figure 2.8 and Figure 2.10) Based on these results we propose a vector strategy that considers the following criteria: Stable transduction should be followed by the selection of a single clone population, to minimize variation of small RNA-mediated gene regulation due to the genomic context. The reporter construct should respond to a single artificial miRNA maximizing the regulatory effect, hence the window of derepression,

enabling solid selection conditions upon mutagenesis. Ultimately the vector strategy should be capable of monitoring reporter derepression as a consequence of small RNA regulation.

Taken together these studies show that genetic manipulation of haploid mESCs enables the characterization of core components of the miRNA pathway. The *Drosha* mutant mESCs line reveals previous identified and novel regulatory freedback-loops of the murine miRNA pathway and opens up the possibility to obtain additional knowledge about the exact regulatory mechanism in an *ex vivo* situation. Furthermore we proposed genetic screen based on reporter for small RNA-mediated gene regulation requires controlled and efficient selection. We propose an inducible two-step reporter setup for a forward genetic screen in haploid mESCs to determine the genetic requirements for the murine small RNA silencing pathway.

# 4 Experimental procedures

## Cell culture

### Thawing, maintenance and freezing of mESCs and NIH3T3 cells.

Cells were thawed at 37°C, at a Temperature of 0°C, and then they were transferred into 10 mL appropriated medium (25 °C) and centrifuged (200 g, 3 min). The supernatant was removed and the cells resuspended in 10 mL appropriated medium and plated in Nunc™ Dishes, Thermo scientific.

For maintenance mESC medium was exchanged everyday. mESCs were passaged every second day and NIH3T3 cells were passaged every third day at 80 % confluence. Medium was removed and cells were washed with 10 mL 1 x PBS for the passaging. The adherent cells were detached using 1 mL of 1 x Trypsin (37 °C, 5 min). Trypsin activity was stoped with 9 mL medium. A single cell suspension created. mESCs were diluted in an 1:15 ratio and NIH3T3 cells in an 1:10 ratio and transferred in a new tissue culture dish.

For long term storage in liquid nitrogen the single cell suspension was centrifuged and the cell pellet resuspended in freezing medium. Cells were frozen in Nunc CryoTube Vials at -80 °C and after 48 h stored in liquid nitrogen.

*NIH3T3 cells medium*

Dulbecco's Modified Eagle's Medium (DMEM), 10 % (v/v) Fetal Bovine Serum heat inactivated 56° C for 45 min, 100 U penicillin/ml, 0.1 mg streptomycin/ml and 2 mM L-Glutamine.

*mESC medium*

DMEM, 15% (v/v), fetal calf serum, 2 mM L- Glutamine, 1 mM sodium pyruvate, 100 U penicillin/ml, 0.1 mg streptomycin/ml, 1x non essential aminoacids, 100 $\mu$M 2-mercoptoethanol and LIF at 1,000 U/ml

*Platinum Retroviral Packaging Cell Line (Plat-E) medium*

Maintenance medium: DMEM, 10 % (v/v) Fetal Bovine Serum heat inactivated 56° C for 45 min, 1 $\mu$g/mL puromycin, 10 $\mu$g/mL blasticidin, 100 U/ml penicillin, 0.1 mg/ml streptomycin and 2 mM L-Glutamine.

*Plat-E Viral production medium:*

DMEM, 10 % (v/v) Fetal Bovine Serum heat inactivated 56° C for 45 min and 2 mM L-Glutamine

## Generation of transgenic mESCs and NIH3T3 cells

### Virus production

Plat-E cells were cultured for two days in in Dulbecco's Modified Eagle's Medium (DMEM), 10 % (v/v) Fetal Bovine Serum heat inactivated 56° C for 45 min and 2 mM L-Glutamine. At 75% confluence Plat-E cells were supplied with fresh medium containing 25 $\mu$M chloroquine and transfected with $CaCl_2$ transfection. Plat-E cells were supplied with target cell medium twelve hours after $CaCl_2$ transfection. Virus containing supernatant was harvested 24 h, 36h and 48 h after transfection. Supernatant was purified through 0.2 $\mu$m filter and virus was concentrated by centrifugation in Amicon Ultra-15 Centrifugal Filter Units at +4° C at 3000 g. Virus was stored at +4° C until usage.

*$CaCl_2$ transfection mixture.*

| | 10 cm dish | 15 cm dish |
|---|---|---|
| Plasmid DNA | 20 $\mu$g | 60 $\mu$g |

| | | | | |
|---|---|---|---|---|
| Plasmid Gag/Pol | 3 | µg | 10 | µg |
| Plasmid shDGCR8 | 1.5 | µg | 5 | µg |
| $CaCl_2$ 2 M | 62.5 | µL | 187.5 | µL |
| $_{dd}$H2O | To 500 | µL | To 1500 | µL |
| 2x HBS | 500 | µL | 1500 | µL |

**Fluorescence activated cell sorting**

Cells were detached with 1x Trypsin and washed once in 1x PBS. Cell were resuspended in 1x PBS and singularized by filtration through a 35 µm cell strainer. Cells were sorted using a BD FACSAria™ III and collected in cell culture medium. Sorted cells were centrifuged for 3 min at 200 g and plated in fresh medium. Medium was exchanged after the cells attached.

**DNA staining with Hoechst**

Single cell suspension was created and nuclear DNA was stained in 30 mL mESC medium with 10 µg bisBenzimide H 33342 trihydrochloride pro mL medium with regular inverting (37 °C, 30 min). Stained cells were resuspended in 1 x PBS for flow cytometry.

**Single cell clone isolation**

2000 mESCs were plated on a 15 cm dish in 30 mL medium. Medium was carefully exchanged five days later and after an additional five days later colonies were picked with a 20 µL pipette and transferred in 96 round bottom wells plate containing 40 µL 1 x PBS. Transferred colony was trypsinized with 20 µL of 3 x Trypsin (37 °C, 10 min). Reaction was stop with 140 µL mESC medium. 40 µL of Single cell suspension was transferred in fresh 96 round bottom wells plate containing 160 µL freezing medium. 96 round bottom wells plates were wrapped with parafilm and aluminum foil and stored at -80 °C.

## Western Blot analysis

### Protein sample preparation

Cell were harvested and washed three times in cold 1x PBS. Washed cells were lysed with passive lysis buffer for 1h at +4 Celsius under constant shaking. Cell debris was removed by centrifugation (20817 g, +4 °C, 1 h). Protein concentration was assayed in technical duplicates with Protein Assay Dye Reagent Concentrate and absorption was determined with BioPhotometer plus.

### SDS-PAGE

Protein samples were denatured in 2x sample loading buffer at 95 °C for 5 min.

Denatured protein samples were separated by size in SDS-PAGE at 200 V in 1x SDS buffer. Polyacrylamide gels were casted according to The Condensed Protocols From Molecular Cloning: A Laboratory Manual by Joseph Sambrook and David William Russell 2006.

### Western Blot

Proteins were blotted on PVDF membrane (30V, +4°C, 12 h) using Mini Trans-Blot Module in 1x transfer buffer. PVDF membrane was blocked in blocking buffer at RT. Antibodies were diluted in blocking buffer and the primary antibody was incubated with the membrane (+4°C, 12 h). Subsequently the membrane was washed three times in TBS-T 0.1% (RT, 10 min). After HRP coupled secondary antibody incubation (RT, 1 h) the membrane was washed again. Protein expression was detected with ImmunStar™ Western C™ Substrate Kit. Image acquisition and quantification were performed in Molecular Imager® Gel Doc™ XR+ System and Image Lab.

Antibodies

| Name | Specificity | Company | Catalog # | Source | Dilutions |
|---|---|---|---|---|---|
| 12G10-anti- | mice | DSHB | | mice | 1:400,000 |

| | | | | | |
|---|---|---|---|---|---|
| alpha-tubulin | | | | | |
| Drosha Antibody 0.1ml | mice | Novus Biologicals | NBP1-03349 | rabbit | 1:1000 |
| Argo2 C34C6 | mice | Cellsignal | 2897S | rabbit | 1:1000 |
| DGCR8 Antibody | mice | Thermo scientific | PA5-18614 | goat | 3:10000 |
| J101-Dicer | mice | Rajewsky | | rabbit | 1:2000 |

## Reverse transcription and real-time-quantitative-PCR (qPCR)

### cDNA synthesis

Total RNA was isolated from cells using mirVana™ miRNA Isolation Kit according to manufacturer's protocol. 12.5 µg of RNA were treated with TurboDNase (37 °C, 1h). TurboDNase was heat inactivated (65 °C, 10 min) and total RNA recovered by Phenol/Chloroform extraction and ethanol precipitation. RNA was converted into cDNA using Superscript III with random hexamer or oligo-$dT_{18}$ primer according to manufacturer's protocol.

### Real-Time-quantitative-PCR (qPCR)

qPCR was performed using 2x qPCR buffer and 0.35 $\mu$M Primer (each) in CFX96 – C1000 Thermal Cycle. The data was analyzed in triplets for Δ-CT values with CFX96 Manager. Results were normalized to β-actin and GAPDH expression.

| DNA digestion | | | qPCR program | | |
|---|---|---|---|---|---|
| Total RNA | 12.5 | $\mu$g | 1x | 95 °C | 3 min |
| 10x Turbo DNase buffer | 5 | $\mu$L | 40x | 95 °C | 15 sec |
| Turbo DNase | 1 | $\mu$L | | 55 °C | 30 sec |
| $H_2O$ | x | $\mu$L | | 72 °C | 30 sec |
| Total Volume | To 50 | $\mu$L | 61x | 65°C + 0.5 °C | 10 sec |

qPCR-Primers

| | |
|---|---|
| Q-mmu-betaactinfwd | CAGAAGGAGATTACTGCTCTGGCT |
| Q-mmu-betaactinrev | TACTCCTGCTTGCTGATCCACATC |
| Q-mmu-GAPDHrev | TGCAGGGATGATGTTCTGGG |
| Q-mmu-GAPDHfwd | TGATGGGTGTGAACCACGAG |
| Q-mmu-Droshafwd | CCAAGATGATCCAACTCCTT |
| Q-mmu-Drosharew | GGTGCTGATTCTGAACAATG |
| Q-mmu-DGCR8fw | TGCCAAGAAGAACAGGCCCAACC |
| Q-mmu-DGCR8rev | TGGCCCATGCTGCCTACCTCATAC |
| Q-mmu-Dicer1fwd | ACCTGACCAATCTCAACCAGC |
| Q-mmu-Dicer1rev | TTTGGCCTTCCTCTTCTCAGC |
| Q-mmu-trbp1+2rev | AGCTCACGCCAATGGAAA |
| Q-mmu-trbp1+2fwd | CGTAACGCAGCAGCTAAGA |
| Q-mmu-pactrev | CTAAGTCGCTCCAAGCCTAC |
| Q-mmu-pactfwd | TCCTCAGTCTCCCGAACAC |
| Q-mmu-Ago1fwd | CTGTGGGCAAACCAATCAAGC |
| Q-mmu-Ago1rev | GCGGTTTGAAATGCTGGACC |
| Q-mmu-Ago2fwd | GCACCACCGGGAGAACAATC |
| Q-mmu-Ago2rev | CAAACACTGGCTTCCGGTCC |
| Q-mmu-Ago3fwd | AGGACTGTCGCCGCTCTTAC |
| Q-mmu-Ago3rev | AGGACTGTCGCCGCTCTTAC |
| Q-mmu-Ago4fwd | CGCTTCAGCGCCAATATTCC |
| Q-mmu-Ago4rev | GTCGAATTGGTTTCCCAACGG |
| Q-mmu- 5' of mir290 rev | AGCTTTGGTTTCTGGTCCCC |
| Q-mmu- 5' of mir290 fwd | TCAAGGGAGGAACGAGCCTA |
| Q-mmu- 3' of mir295 fwd | TCCTGCCCAGTAGACGGTAA |
| Q-mmu- 3' of mir295 rev | TAACAGCTCCAAGCAGCGAC |
| Q-mmu-3' of miR96fwd | GTGAGGAGGGTACAGCCCTA |

| | |
|---|---|
| Q-mmu-3' of miR96rev | TAAGGAGGAGGAGCCCAACA |
| Q-mmu-5' of miR135bfwd | GGCGTCTTGAAAGGATTGCC |
| Q-mmu-5' of miR135rev | GGAACGCATTCTCTCACCGT |
| Q-mmu-5' of miR182fwd | CTGAGGCCACAAGGAAGTGT |
| Q-mmu-5' of miR182rev | GACCTCAACACACTCCGTCC |
| Q-mmu-miR135b preRNAfwd | GGAGACGGTGAGAGAATGCG |
| Q-mmu-miR135b premiRNArev | TCCAAGCCAGGCCTCAAAAA |
| Q-miR182premirRNArev | GACAGGAGTCCCCTCTCCTT |
| Q-miR182premirRNAfwd | GGCCGAAGGACCATAGTCTG |
| Q-miR96premirRNArev | CCCAGCAGTAAGCCAGATG |
| Q-miR96premirRNAfwd | TTTCTGCCTAGACCTCTGTTTC |
| Q-miR295premiRNArev | TACACATGCATGAAAGCAGCC |
| Q-miR295premiRNAfwd | GAGACTCCTTGCTTGCTCATC |
| Q-miR294premirRNArev | TGAGCAAGCAAGGAGTCTCTG |
| Q-miR294premirRNAfwd | CGGGAAGTGACCCAGATTTGA |
| Q-miR293premirRNArev | TCCGTGCACCTCAGCTTTTA |
| Q-miR293premirRNAfwd | AGGTCCCTGTGGAAATGCTT |
| Q-miR292premirRNArev | CACCTGCCCAGAAATGCAAC |
| Q-miR292premirRNAfwd | CGAGACGCGGATGGATGTAA |
| Q-miR291bpremirRNArev | GCAGGTAAGCGATTCCAGGT |
| Q-miR291bpremirRNAfwd | CGTTCATAAAGGAGCCGGGA |
| Q-miR291apremirRNArev | AAGCCTAAACCCCCACACAG |
| Q-miR291apremirRNAfwd | GACGGTAACTGAGGTGGTCG |
| Q-miR290premirRNArev | ACCCTACAACGACCACCTCA |
| Q-miR290premirRNAfwd | GTTTTAACGTCTGGACCGCC |

## Northern Blot analysis

### Denaturing polyacrylamide gel electrophoresis

6 $\mu$g total RNA, prepared using the miRVANA kit, were diluted in 2 x Gel Loading Buffer II and denatured (95 °C, 5 min). Denatured RNA was loaded in rinsed well of denaturing polyacrylamide gel with a temperature of 50 °C. Small RNAs were separated in a 15% denaturing polyacrylamide gel by electrophoresis (80 W, 2 h).

### Northern Blot

Small RNAs (19 – 23 nt) and loading control (U6 snRNP, 106 nt) were transferred under semi dry conditions on Hybond-NX or Amersham Hybond N+ membrane, (20 V, 1 h), respectively. Small RNAs were crosslinked to membrane with EDC solution (60 °C, 1h), whereas UV-crosslinking (2 x 120 mJ, **λ =** 254 nm) was applied for the loading control.

Crosslinked RNA was incubated in church buffer (60 °C, 1 h) and 32P labeled northern probes were hybridized to RNA (37 °C, 12 h) in church buffer. Excessive northern probes were washed away with 1 x SSC washing buffer (3 x, 37 °C, 10 min). Beta radiation was captured on storage phosphor screen and the latent image was scanned at 100 $\mu$m using a Typhoon Trio. The signal intensity was quantified with ImageQuant TL. SmallRNA were normalized to loading control.

### Northern probe labeling

DNA oligonucleotides, reverse complement to the target small RNA, were labeled on the 5´ -hydroxyl terminus with 32- $P_i$ (37 °C, 1 h) and purified on Illustra G25 MicroSpin columns.

Northern probe labbeling

| | | |
|---|---|---|
| DNA Probe (25 $\mu$M) | 1 | $\mu$L |
| T4-PNK buffer | 3 | $\mu$L |

| | | |
|---|---|---|
| γ-32P-ATP (25 μM) | 3 | μL |
| PNK | 1 | μL |
| $H_2O$ | 22 | μL |
| Total Volume | To 30 | μL |

| | |
|---|---|
| NP-mmu-mir-135b | TCACATAGGAATGAAAAGCCATA |
| NP-mmu-miR-136-5p | CCATCATCAAAACAAATGGAGT |
| NP-mmu-miR-182-5p | CGGTGTGAGTTCTACCATTGCCAAA |
| NP-mmu-mir-290-5p | AAAGTGCCCCCATAGTTTGAGT |
| NP-mmu-mir-291a-3p | AGAGAGGGCCTCCACTTTGATG |
| NP-mmu-mir-291b-3p | ACAAACAAAATGGATGCACTTT |
| NP-mmu-miR-291b-5p | GGAGAGGGCCTCCACTTTGATC |
| NP-mmu-miR-292-3p | ACACTCAAAACCTGGCGGCACTTT |
| NP-mmu-miR-294-3p | ACACACAAAAGGGAAGCACTTT |
| NP-mmu-miR-295-3p | AGACTCAAAAGTAGTAGCACTTT |
| NP-mmu-miR-96-5p | AGCAAAAATGTGCTAGTGCCAAA |
| NP-mmu-miR19b | TCAGTTTTGCATGGATTTGCACA |
| NP-mmu-miR293 | ACACTACAAACTCTGCGGCACT |
| NP-U6-snRNA | GCTTCACGAATTTGCGTGTCATCCT |

## Cloning

### Endogenous miRNA reporter construct

An endogenous miRNA reporter construct was generated for a reporter cell line for miRNA function. pSIN Venus p2a Puromycin miRBS1 EF1a mCherry was a product of several cloning steps.

In the first step pSIN PGK Venus was generated. The PGK promoter of pSIN PGK Cre-ER$^{T2}$-IRES-Neomycin was introduced into pSIN TRE tight Neomycin miR-30 PGK Venus (both vectors were kind gifts of the Zuber laboratory). Both

plasmids were digested with AgeI and BglII. The PGK promoter from pSIN PGK Cre-ER$^{T2}$-IRES-Neomycin was gel purified. TRE tight Neomycin miR-30 PGK was removed from pSIN TRE tight Neomycin miR-30 PGK Venus and pSIN Venus backbone was gel purified and dephosphorylated. The ligation was performed and the resulting pSIN PGK Venus plasmid was sequenced to verify the insertion.

In the second step the stop-codon of Venus was removed by site-directed mutagenesis. A PCR with antiparallel primers overlapping at the stop-codon of pSIN Venus created a linear ds copy of pSIN Venus with a three nucleotide change at the taa stop codon to gga glycin. Before the transformation DpnI digested the template DNA, pSIN Venus. pSIN Venus noStop was sequenced to exclude mutations.

VenusNoStopCF15-Fwd: TGTACAAGGGAGAATTGTTCAATTACGCGTAC

VenusNoStop-Rev: GAACAATTCTCCCTTGTACAGCTCGTCCAT

In the third step the p2a and multiple cloning sites were integrated. A 176 nucleotide long dsDNA gBlock from IDT was ordered. The gBlock was KOD PCR amplified. The gel purified PCR product and pSIN Venus noStop were digested with MluI and EcoRV for directional cloning. After gel purification digested pSIN Venus no Stop was dephosphorylated and ligated to the digested gBlock. The ligation product pSIN Venus no Stop gBlock was sequenced to verify integration and exclude mutations.

CAGGS-Fwd: CTGCTGTCCATTCCTTATTC

CAGGS-Rev: CATGTCAACCAGAGTTT

In the fourth step the puromycin resistance was integrated into pSIN Venus no Stop gBlock to generate pSIN Venus p2a Puro. The puromycin resistance gene was PCR amplified with primers containing BamHI and EcoRI restriction sites. pSIN Venus no Stop gBlock and the PCR amplicon were digested with BamHI

and EcoRI. After Backbone dephosphorylation the ligation was performed. The product pSIN PGK Venus p2a Puro (PVnsgBP) was sequenced to verify integration and exclude mutations.

PuroBamHiEcoRI-Fwd : ATGCATGGATCCATGACCGAGTACAAGCCCAC

PuroBamHiEcoRI-Rev: ACAGTCGAATTCTCAGGCACCGGGCTTGC

In the fifth step the second promoter (EF1a) and the control fluorophore (mCherry) were integrated into pSIN PGK Venus p2a Puro to generate pSIN Venus p2a Puro EF1a mCherry. The EF1a mCherry cassette was PCR amplified with primers containing HpaI and NotI restriction sites. pSIN PGK Venus p2a Puro and the PCR product were digested with HpaI and NotI. After Backbone dephosphorylation the ligation was performed. The product pSIN Venus p2a Puro EF1a mCherry was sequenced to verify integration and exclude mutations.

EF1amCherryHpaINotI-Fwd:
GCATGCGTGTTAACCGAGAAGCTTGATCGATGGC

HpaIEF1amCherryNotIstop-rev:
CGATGCAGCGGCCGCTTACTTGTACAGCTCGTCCATG

In the sixth step the miRBS1 was integrated in pSIN Venus p2a Puro EF1a mCherry to generate the endogenous miRNA reporter construct. miRBS1 contains five full complementary sites (miR-135b, miR-19b, miR-291b, miR-19b and miR-135b). The miRBS1 was PCR amplified from a 393-nucleotide dsDNA strand synthesis by IDT (gBLockmiRBScanonicalindependen). The PCR amplicon and the pSIN Venus p2a Puro EF1a mCherry backbone were digested with the restriction enzymes XbaI and XhoI. After the dephosphorylation of the backbone the ligation was performed. The ligation product pSIN Venus p2a Puro miRBS1 EF1a mCherry (PVp2aPmiRBS1EmC) were sequenced to verify integration and exclude mutations.

CAGGS-Fwd: CTGCTGTCCATTCCTTATTC

CAGGS-Rev: CATGTCAACCAGAGTTT

**shRNA reporter construct**

An shRNA expressing reporter construct was generated to establish a reporter cell line for small RNA function. The inducible TRE3G promoter of pSIN TRE3G turbo GFP miR-E EF1a mCherry p2a Blasticidin 4xmiR-E binding site (T3tGmEECB4xEBS) (a gift from the Zuber laboratory) was exchanged with a constitutive PGK promoter. The TRE3G promoter of T3tGmEECB4x713 was removed with the restriction enzymes XbaI and DamHI. The Backbone was dephosphorylated and gel purified. The PGK promoter of the PGK Venus p2a Puromycin miRBS1 EF1a mCherry was PCR amplified with primers containing XbaI and DamHI restriction sites for directional cloning. The PCR amplicon was gel purified and digested with XbaI and DamHI. The digested PCR amplicon was gel purified and ligated with the dephosphorylated Backbone. pSIN PGK turboGFP miR-E EF1a mCherry p2a Blasticidin 4xmiR-E binding site (PtGmEECB4xEBS) was sequenced to exclude mutations.

**Bacteria transformation**

50 $\mu$L of chemical competent DH5-α bacteria were thawed on ice and 50 ng of plasmid DNA was added. Subsequently bacteria were heatshocked (42 °C, 1 min) and transferred back to ice for one min. 250 $\mu$L of SOC were added and bacteria grown (37 °C, 1 h). Finally 100 $\mu$L of bacteria suspension was plated on agar plate containing the appropriate antibiotic and incubated (shaking, 37 °C, 1 h).

**Plasmid DNA preparation for transfection or subcloning**

For transfection plasmid DNA of high purity was obtained using the Qiagen plasmid maxi kit. A bacteria colony was inoculated in 250 mL LB medium containing the appropriate antibiotic and grown for 12 h. Subsequently plasmid DNA was prepared according to manufacture protocol.

For subcloning, plasmid DNA was obtain in small scale using the QIAprep Spin Miniprep Kit according to manufacture protocol.

**Plasmid DNA restriction digest**

Plasmid DNA was digested with appropriated restriction enzymes (37 °C, 3 h). Backbone DNA fragments were additionally dephosphorylated using thermosensitive alkaline phosphatase (37 °C, 1 h). The desired DNA fragment was size separated by agarose gel electrophoresis (120 V, 40 min). DNA fragment was excised from agarose gel and using Wizard® SV Gel and PCR Clean-Up System.

| Plasmid DNA restriction digest | | | Backbone DNA dephosphorylation | | |
|---|---|---|---|---|---|
| Plasmid DNA (1 µg/µL) | 5 | µL | Backbone DNA | 40 | µL |
| FastDigest Green Buffer | 4 | µL | FastDigest Green Buffer | 1 | µL |
| Restriction Enzyme(s) | 4 | µL | FastAP | 1 | µL |
| $H_2O$ | 27 | µL | Thermosensitive | | |
| Total Volumne | 40 | µL | Alkaline Phosphatase | | |
| | | | $H_2O$ | 8 | µL |
| | | | Total Volumne | 50 | µL |

**DNA Ligation**

Backbone DNA and insert DNA were ligated in a molar ration 1 : 3 using a T4-DNA ligase (16 °C, 12 h). Ligation mixture was transformed into DH5-α.

| DNA Ligation | | |
|---|---|---|
| Backbone DNA | 150 | ng |
| Insert DNA | x | ng |
| (3 x mol of backbone DNA) | | |
| 10X Reaction Buffer | 1 | µL |
| T4 DNA Ligase | 0.5 | µL |
| $H_2O$ | To 10 | µL |

| | | |
|---|---|---|
| Total Volume | 10 | μL |

**Transient plasmid transfection**

5000 mES cells were seeded in one well of a Lab-Tek® II Slide, 8 Chamber in 300 μL mESC medium. On the next day a transfection mixture was prepared and 15 min later added to the cells. 48 h after transfection medium was changed to riboflavin and phenol red free DMEM and images were acquired.

DNA Ligation

| | | |
|---|---|---|
| Plasmid DNA | 150 | ng |
| X-tremeGENE 9 | 0.45 | μL |
| Opti-MEM® | 15 | μL |

# Bibliography


Aravin, A., Gaidatzis, D., Pfeffer, S., Lagos-Quintana, M., Landgraf, P., Iovino, N., Morris, P., Brownstein, M.J., Kuramochi-Miyagawa, S., Nakano, T., et al. (2006). A novel class of small RNAs bind to MILI protein in mouse testes. Nature *442*, 203–207.

Auyeung, V.C., Ulitsky, I., McGeary, S.E., and Bartel, D.P. (2013). Beyond secondary structure: primary-sequence determinants license pri-miRNA hairpins for processing. Cell *152*, 844–858.

Axtell, M.J., Westholm, J.O., and Lai, E.C. (2011). Vive la différence: biogenesis and evolution of microRNAs in plants and animals. Genome Biol. *12*, 221.

Babiarz, J.E., Ruby, J.G., Wang, Y., Bartel, D.P., and Blelloch, R. (2008). Mouse ES cells express endogenous shRNAs, siRNAs, and other Microprocessor-independent, Dicer-dependent small RNAs. Genes Dev. *22*, 2773–2785.

Baek, D., Villén, J., Shin, C., Camargo, F.D., Gygi, S.P., and Bartel, D.P. (2008). The impact of microRNAs on protein output. Nature *455*, 64–71.

Bartel, D.P. (2004). MicroRNAs: genomics, biogenesis, mechanism, and function. Cell *116*, 281–297.

Baskerville, S., and Bartel, D.P. (2005). Microarray profiling of microRNAs reveals frequent coexpression with neighboring miRNAs and host genes. Rna *11*, 241–247.

Berezikov, E., Chung, W.-J., Willis, J., Cuppen, E., and Lai, E.C. (2007). Mammalian mirtron genes. Mol. Cell *28*, 328–336.

Bogerd, H.P., Karnowski, H.W., Cai, X., Shin, J., Pohlers, M., and Cullen, B.R. (2010). A mammalian herpesvirus uses noncanonical expression and processing mechanisms to generate viral MicroRNAs. Mol. Cell *37*, 135–142.

Bosher, J.M., and Labouesse, M. (2000). RNA interference: genetic wand and genetic watchdog. Nat. Cell Biol. *2*, E31–E36.

Boutros, M., Kiger, A.A., Armknecht, S., Kerr, K., Hild, M., Koch, B., Haas, S.A., Paro, R., Perrimon, N., Heidelberg Fly Array Consortium (2004). Genome-wide RNAi analysis of growth and viability in Drosophila cells. Science *303*, 832–835.

Brameier, M., Herwig, A., Reinhardt, R., Walter, L., and Gruber, J. (2011). Human box C/D snoRNAs with miRNA like functions: expanding the range of regulatory RNAs. Nucleic Acids Res. *39*, 675–686.

Braun, J.E., Huntzinger, E., Fauser, M., and Izaurralde, E. (2011). GW182 proteins directly recruit cytoplasmic deadenylase complexes to miRNA targets. Mol. Cell *44*, 120–133.

Brennecke, J., Aravin, A.A., Stark, A., Dus, M., Kellis, M., Sachidanandam, R., and Hannon, G.J. (2007). Discrete small RNA-generating loci as master regulators of transposon activity in Drosophila. Cell *128*, 1089–1103.

Brennecke, J., Stark, A., Russell, R.B., and Cohen, S.M. (2005). Principles of microRNA-target

recognition. PLoS Biol. *3*, e85.

Calabrese, J.M., Seila, A.C., Yeo, G.W., and Sharp, P.A. (2007). RNA sequence analysis defines Dicer's role in mouse embryonic stem cells. Proc. Natl. Acad. Sci. U.S.a. *104*, 18097–18102.

Cheloufi, S., Santos, Dos, C.O., Chong, M.M.W., and Hannon, G.J. (2010). A dicer-independent miRNA biogenesis pathway that requires Ago catalysis. Nature *465*, 584–589.

Cherry, S.R., Biniszkiewicz, D., van Parijs, L., Baltimore, D., and Jaenisch, R. (2000). Retroviral expression in embryonic stem cells and hematopoietic stem cells. Mol. Cell. Biol. *20*, 7419–7426.

Chiang, H.R., Schoenfeld, L.W., Ruby, J.G., Auyeung, V.C., Spies, N., Baek, D., Johnston, W.K., Russ, C., Luo, S., Babiarz, J.E., et al. (2010). Mammalian microRNAs: experimental evaluation of novel and previously annotated genes. Genes Dev. *24*, 992–1009.

Chong, M.M.W., Rasmussen, J.P., Rudensky, A.Y., Rundensky, A.Y., and Littman, D.R. (2008). The RNAseIII enzyme Drosha is critical in T cells for preventing lethal inflammatory disease. J. Exp. Med. *205*, 2005–2017.

Cifuentes, D., Xue, H., Taylor, D.W., Patnode, H., Mishima, Y., Cheloufi, S., Ma, E., Mane, S., Hannon, G.J., Lawson, N.D., et al. (2010). A novel miRNA processing pathway independent of Dicer requires Argonaute2 catalytic activity. Science *328*, 1694–1698.

Czech, B., Malone, C.D., Zhou, R., Stark, A., Schlingeheyde, C., Dus, M., Perrimon, N., Kellis, M., Wohlschlegel, J.A., Sachidanandam, R., et al. (2008). An endogenous small interfering RNA pathway in Drosophila. Nature *453*, 798–802.

De-Zolt, S., Altschmied, J., Ruiz, P., Melchner, von, H., and Schnütgen, F. (2009). Gene-trap vectors and mutagenesis. Methods Mol. Biol. *530*, 29–47.

Denli, A.M., Tops, B.B.J., Plasterk, R.H.A., Ketting, R.F., and Hannon, G.J. (2004). Processing of primary microRNAs by the Microprocessor complex. Nature *432*, 231–235.

Dow, L.E., Premsrirut, P.K., Zuber, J., Fellmann, C., McJunkin, K., Miething, C., Park, Y., Dickins, R.A., Hannon, G.J., and Lowe, S.W. (2012). A pipeline for the generation of shRNA transgenic mice. Nat Protoc *7*, 374–393.

Echeverri, C.J., and Perrimon, N. (2006). High-throughput RNAi screening in cultured cells: a user's guide. Nat. Rev. Genet. *7*, 373–384.

Elbashir, S.M., Harborth, J., Lendeckel, W., Yalcin, A., Weber, K., and Tuschl, T. (2001). Duplexes of 21-nucleotide RNAs mediate RNA interference in cultured mammalian cells. Nature *411*, 494–498.

Elling, U., Taubenschmid, J., Wirnsberger, G., O'Malley, R., Demers, S.-P., Vanhaelen, Q., Shukalyuk, A.I., Schmauss, G., Schramek, D., Schnuetgen, F., et al. (2011). Forward and reverse genetics through derivation of haploid mouse embryonic stem cells. Cell Stem Cell *9*, 563–574.

Eppig, J.T., and Strivens, M. (1999). Finding a mouse: the International Mouse Strain Resource (IMSR). Trends Genet. *15*, 81–82.

Eulalio, A., Tritschler, F., and Izaurralde, E. (2009). The GW182 protein family in animal cells: new insights into domains required for miRNA-mediated gene silencing. Rna *15*, 1433–1442.

Evdokimov, A.G., Pokross, M.E., Egorov, N.S., Zaraisky, A.G., Yampolsky, I.V., Merzlyak, E.M., Shkoporov, A.N., Sander, I., Lukyanov, K.A., and Chudakov, D.M. (2006). Structural basis for the fast maturation of Arthropoda green fluorescent protein. EMBO Rep. *7*, 1006–1012.

Eystathioy, T., Jakymiw, A., Chan, E.K.L., Séraphin, B., Cougot, N., and Fritzler, M.J. (2003). The GW182 protein colocalizes with mRNA degradation associated proteins hDcp1 and hLSm4 in cytoplasmic GW bodies. Rna *9*, 1171–1173.

Fabian, M.R., and Sonenberg, N. (2012). The mechanics of miRNA-mediated gene silencing: a look under the hood of miRISC. Nat. Struct. Mol. Biol. *19*, 586–593.

Fabian, M.R., Sonenberg, N., and Filipowicz, W. (2010). Regulation of mRNA translation and stability by microRNAs. Annu. Rev. Biochem. *79*, 351–379.

Fellmann, C., Zuber, J., McJunkin, K., Chang, K., Malone, C.D., Dickins, R.A., Xu, Q., Hengartner, M.O., Elledge, S.J., Hannon, G.J., et al. (2011). Functional identification of optimized RNAi triggers using a massively parallel sensor assay. Mol. Cell *41*, 733–746.

Forman, J.J., Legesse-Miller, A., and Coller, H.A. (2008). A search for conserved sequences in coding regions reveals that the let-7 microRNA targets Dicer within its coding sequence. Proc. Natl. Acad. Sci. U.S.a. *105*, 14879–14884.

Friedman, A., and Perrimon, N. (2004). Genome-wide high-throughput screens in functional genomics. Curr. Opin. Genet. Dev. *14*, 470–476.

Ghildiyal, M., and Zamore, P.D. (2009). Small silencing RNAs: an expanding universe. Nat. Rev. Genet. *10*, 94–108.

Ghildiyal, M., Seitz, H., Horwich, M.D., Li, C., Du, T., Lee, S., Xu, J., Kittler, E.L.W., Zapp, M.L., Weng, Z., et al. (2008). Endogenous siRNAs derived from transposons and mRNAs in Drosophila somatic cells. Science *320*, 1077–1081.

Giegé, R. (2008). Toward a more complete view of tRNA biology. Nat. Struct. Mol. Biol. *15*, 1007–1014.

Girard, A., Sachidanandam, R., Hannon, G.J., and Carmell, M.A. (2006). A germline-specific class of small RNAs binds mammalian Piwi proteins. Nature *442*, 199–202.

Golden, D.E., Gerbasi, V.R., and Sontheimer, E.J. (2008). An inside job for siRNAs. Mol. Cell *31*, 309–312.

Gregory, R.I., Yan, K.-P., Amuthan, G., Chendrimada, T., Doratotaj, B., Cooch, N., and Shiekhattar, R. (2004). The Microprocessor complex mediates the genesis of microRNAs. Nature *432*, 235–240.

Griffiths-Jones, S. (2004). The microRNA Registry. Nucleic Acids Res. *32*, D109–D111.

Grimm, S. (2004). The art and design of genetic screens: mammalian culture cells. Nat. Rev. Genet. *5*, 179–189.

Grimson, A., Farh, K.K.-H., Johnston, W.K., Garrett-Engele, P., Lim, L.P., and Bartel, D.P. (2007). MicroRNA targeting specificity in mammals: determinants beyond seed pairing. Mol. Cell *27*, 91–105.

Guil, S., and Cáceres, J.F. (2007). The multifunctional RNA-binding protein hnRNP A1 is required for processing of miR-18a. Nat. Struct. Mol. Biol. *14*, 591–596.

Guo, H., Ingolia, N.T., Weissman, J.S., and Bartel, D.P. (2010). Mammalian microRNAs predominantly act to decrease target mRNA levels. Nature *466*, 835–840.

Han, J., Lee, Y., Yeom, K.-H., Nam, J.-W., Heo, I., Rhee, J.-K., Sohn, S.Y., Cho, Y., Zhang, B.-T., and Kim, V.N. (2006). Molecular basis for the recognition of primary microRNAs by the Drosha-DGCR8 complex. Cell *125*, 887–901.

Han, J., Lee, Y., Yeom, K.-H., Kim, Y.-K., Jin, H., and Kim, V.N. (2004). The Drosha-DGCR8 complex in primary microRNA processing. Genes Dev. *18*, 3016–3027.

Han, J., Pedersen, J.S., Kwon, S.C., Belair, C.D., Kim, Y.-K., Yeom, K.-H., Yang, W.-Y., Haussler, D., Blelloch, R., and Kim, V.N. (2009). Posttranscriptional crossregulation between Drosha and DGCR8. Cell *136*, 75–84.

Hansen, G.M., Markesich, D.C., Burnett, M.B., Zhu, Q., Dionne, K.M., Richter, L.J., Finnell, R.H., Sands, A.T., Zambrowicz, B.P., and Abuin, A. (2008). Large-scale gene trapping in C57BL/6N mouse embryonic stem cells. Genome Res. *18*, 1670–1679.

Hansen, J., Floss, T., Van Sloun, P., Füchtbauer, E.-M., Vauti, F., Arnold, H.-H., Schnütgen, F., Wurst, W., Melchner, von, H., and Ruiz, P. (2003). A large-scale, gene-driven mutagenesis approach for the functional analysis of the mouse genome. Proc. Natl. Acad. Sci. U.S.a. *100*, 9918–9922.

Haussecker, D. (2012). The Business of RNAi Therapeutics in 2012. Mol Ther Nucleic Acids *1*, e8.

Haussecker, D., Huang, Y., Lau, A., Parameswaran, P., Fire, A.Z., and Kay, M.A. (2010). Human tRNA-derived small RNAs in the global regulation of RNA silencing. Rna *16*, 673–695.

Heo, I., Joo, C., Cho, J., Ha, M., Han, J., and Kim, V.N. (2008). Lin28 mediates the terminal uridylation of let-7 precursor MicroRNA. Mol. Cell *32*, 276–284.

Huang, Y., and Steitz, J.A. (2001). Splicing factors SRp20 and 9G8 promote the nucleocytoplasmic export of mRNA. Mol. Cell *7*, 899–905.

Huntzinger, E., and Izaurralde, E. (2011). Gene silencing by microRNAs: contributions of translational repression and mRNA decay. Nat. Rev. Genet. *12*, 99–110.

Hutvágner, G., McLachlan, J., Pasquinelli, A.E., Bálint, E., Tuschl, T., and Zamore, P.D. (2001). A cellular function for the RNA-interference enzyme Dicer in the maturation of the let-7 small temporal RNA. Science *293*, 834–838.

Iwasaki, S., Kobayashi, M., Yoda, M., Sakaguchi, Y., Katsuma, S., Suzuki, T., and Tomari, Y. (2010). Hsc70/Hsp90 chaperone machinery mediates ATP-dependent RISC loading of small RNA duplexes. Mol. Cell *39*, 292–299.

Johnston, M., Geoffroy, M.-C., Sobala, A., Hay, R., and Hutvagner, G. (2010). HSP90 protein stabilizes unloaded argonaute complexes and microscopic P-bodies in human cells. Mol. Biol. Cell *21*, 1462–1469.

Karginov, F.V., Cheloufi, S., Chong, M.M.W., Stark, A., Smith, A.D., and Hannon, G.J. (2010). Diverse endonucleolytic cleavage sites in the mammalian transcriptome depend upon microRNAs, Drosha, and additional nucleases. Mol. Cell *38*, 781–788.

Kaspi, H., Chapnik, E., Levy, M., Beck, G., Hornstein, E., and Soen, Y. (2013). miR--290--295 Regulate Embryonic Stem Cell Differentiation Propensities by Repressing Pax6. Stem Cells.

Kawamata, T., and Tomari, Y. (2010). Making RISC. Trends Biochem. Sci. *35*, 368–376.

Kennerdell, J.R., and Carthew, R.W. (1998). Use of dsRNA-mediated genetic interference to demonstrate that frizzled and frizzled 2 act in the wingless pathway. Cell *95*, 1017–1026.

Kile, B.T., and Hilton, D.J. (2005). The art and design of genetic screens: mouse. Nat. Rev. Genet. *6*, 557–567.

Kim, J.H., Lee, S.-R., Li, L.-H., Park, H.-J., Park, J.-H., Lee, K.Y., Kim, M.-K., Shin, B.A., and Choi, S.-Y. (2011). High cleavage efficiency of a 2A peptide derived from porcine teschovirus-1 in human cell lines, zebrafish and mice. PLoS ONE *6*, e18556.

Kim, Y.-K., and Kim, V.N. (2007). Processing of intronic microRNAs. Embo J. *26*, 775–783.

Kiss, T. (2002). Small nucleolar RNAs: an abundant group of noncoding RNAs with diverse cellular functions. Cell *109*, 145–148.

Kühn, R., and Torres, R.M. (2002). Cre/loxP recombination system and gene targeting. Methods Mol. Biol. *180*, 175–204.

Lagos-Quintana, M., Rauhut, R., Lendeckel, W., and Tuschl, T. (2001). Identification of novel genes coding for small expressed RNAs. Science *294*, 853–858.

Lau, N.C., Lim, L.P., Weinstein, E.G., and Bartel, D.P. (2001). An abundant class of tiny RNAs with probable regulatory roles in Caenorhabditis elegans. Science *294*, 858–862.

Lee, R.C., and Ambros, V. (2001). An extensive class of small RNAs in Caenorhabditis elegans. Science *294*, 862–864.

Lee, R.C., Feinbaum, R.L., and Ambros, V. (1993). The C. elegans heterochronic gene lin-4 encodes small RNAs with antisense complementarity to lin-14. Cell *75*, 843–854.

Lee, Y.S., Shibata, Y., Malhotra, A., and Dutta, A. (2009). A novel class of small RNAs: tRNA-derived RNA fragments (tRFs). Genes Dev. *23*, 2639–2649.

Lee, Y., Ahn, C., Han, J., Choi, H., Kim, J., Yim, J., Lee, J., Provost, P., Rådmark, O., Kim, S., et al. (2003). The nuclear RNase III Drosha initiates microRNA processing. Nature *425*, 415–419.

Lee, Y., Hur, I., Park, S.-Y., Kim, Y.-K., Suh, M.R., and Kim, V.N. (2006). The role of PACT in the RNA silencing pathway. Embo J. *25*, 522–532.

Lee, Y., Jeon, K., Lee, J.-T., Kim, S., and Kim, V.N. (2002). MicroRNA maturation: stepwise processing and subcellular localization. Embo J. *21*, 4663–4670.

Lee, Y., Kim, M., Han, J., Yeom, K.-H., Lee, S., Baek, S.H., and Kim, V.N. (2004a). MicroRNA genes are transcribed by RNA polymerase II. Embo J. *23*, 4051–4060.

Lee, Y.S., Nakahara, K., Pham, J.W., Kim, K., He, Z., Sontheimer, E.J., and Carthew, R.W. (2004b). Distinct roles for Drosophila Dicer-1 and Dicer-2 in the siRNA/miRNA silencing pathways. Cell *117*, 69–81.

Leeb, M., and Wutz, A. (2011). Derivation of haploid embryonic stem cells from mouse embryos. Nature *479*, 131–134.

Leung, A.K.L., Vyas, S., Rood, J.E., Bhutkar, A., Sharp, P.A., and Chang, P. (2011). Poly(ADP-ribose) regulates stress responses and microRNA activity in the cytoplasm. Mol. Cell *42*, 489–499.

Li, H., Li, W.X., and Ding, S.W. (2002). Induction and suppression of RNA silencing by an animal virus. Science *296*, 1319–1321.

Liu, J., Carmell, M.A., Rivas, F.V., Marsden, C.G., Thomson, J.M., Song, J.-J., Hammond, S.M., Joshua-Tor, L., and Hannon, G.J. (2004). Argonaute2 is the catalytic engine of mammalian RNAi. Science *305*, 1437–1441.

Luo, G., Santoro, I.M., McDaniel, L.D., Nishijima, I., Mills, M., Youssoufian, H., Vogel, H., Schultz, R.A., and Bradley, A. (2000). Cancer predisposition caused by elevated mitotic recombination in Bloom mice. Nat. Genet. *26*, 424–429.

MacRae, I.J., Ma, E., Zhou, M., Robinson, C.V., and Doudna, J.A. (2008). In vitro reconstitution of the human RISC-loading complex. Proc. Natl. Acad. Sci. U.S.a. *105*, 512–517.

MacRae, I.J., Zhou, K., and Doudna, J.A. (2007). Structural determinants of RNA recognition and cleavage by Dicer. Nat. Struct. Mol. Biol. *14*, 934–940.

MacRae, I.J., Zhou, K., Li, F., Repic, A., Brooks, A.N., Cande, W.Z., Adams, P.D., and Doudna, J.A. (2006). Structural basis for double-stranded RNA processing by Dicer. Science *311*, 195–198.

Martinez, J., and Tuschl, T. (2004). RISC is a 5' phosphomonoester-producing RNA endonuclease. Genes Dev. *18*, 975–980.

Martinez, N.J., and Gregory, R.I. (2013). Argonaute2 expression is post-transcriptionally coupled to microRNA abundance. Rna *19*, 605–612.

Mathonnet, G., Fabian, M.R., Svitkin, Y.V., Parsyan, A., Huck, L., Murata, T., Biffo, S., Merrick, W.C., Darzynkiewicz, E., Pillai, R.S., et al. (2007). MicroRNA inhibition of translation initiation in vitro by targeting the cap-binding complex eIF4F. Science *317*, 1764–1767.

McKusick, V.A., and Chase, G.A. (1973). Human genetics. Annu. Rev. Genet. *7*, 435–472.

Meister, G. (2013). Argonaute proteins: functional insights and emerging roles. Nat. Rev. Genet. *14*, 447–459.

Meister, G., Landthaler, M., Patkaniowska, A., Dorsett, Y., Teng, G., and Tuschl, T. (2004). Human Argonaute2 mediates RNA cleavage targeted by miRNAs and siRNAs. Mol. Cell *15*, 185–197.

Mello, C.C., and Conte, D. (2004). Revealing the world of RNA interference. Nature *431*, 338–342.

Melo, S.A., Ropero, S., Moutinho, C., Aaltonen, L.A., Yamamoto, H., Calin, G.A., Rossi, S., Fernandez, A.F., Carneiro, F., Oliveira, C., et al. (2009). A TARBP2 mutation in human cancer impairs microRNA processing and DICER1 function. Nat. Genet. *41*, 365–370.

Meyer, L.R., Zweig, A.S., Hinrichs, A.S., Karolchik, D., Kuhn, R.M., Wong, M., Sloan, C.A., Rosenbloom, K.R., Roe, G., Rhead, B., et al. (2013). The UCSC Genome Browser database: extensions and updates 2013. Nucleic Acids Res. *41*, D64–D69.

Mullokandov, G., Baccarini, A., Ruzo, A., Jayaprakash, A.D., Tung, N., Israelow, B., Evans, M.J., Sachidanandam, R., and Brown, B.D. (2012). High-throughput assessment of microRNA activity and function using microRNA sensor and decoy libraries. Nat. Methods *9*, 840–846.

Murchison, E.P., Partridge, J.F., Tam, O.H., Cheloufi, S., and Hannon, G.J. (2005). Characterization of Dicer-deficient murine embryonic stem cells. Proc. Natl. Acad. Sci. U.S.a. *102*, 12135–12140.

Nagy, A., Gócza, E., Diaz, E.M., Prideaux, V.R., Iványi, E., Markkula, M., and Rossant, J. (1990). Embryonic stem cells alone are able to support fetal development in the mouse. Development *110*, 815–821.

Navarro, P., Festuccia, N., Colby, D., Gagliardi, A., Mullin, N.P., Zhang, W., Karwacki-Neisius, V., Osorno, R., Kelly, D., Robertson, M., et al. (2012). OCT4/SOX2-independent Nanog autorepression modulates heterogeneous Nanog gene expression in mouse ES cells. Embo J. *31*, 4547–4562.

Newman, M.A., Thomson, J.M., and Hammond, S.M. (2008). Lin-28 interaction with the Let-7 precursor loop mediates regulated microRNA processing. Rna *14*, 1539–1549.

O'Gorman, S., Fox, D.T., and Wahl, G.M. (1991). Recombinase-mediated gene activation and site-specific integration in mammalian cells. Science *251*, 1351–1355.

Okada, C., Yamashita, E., Lee, S.J., Shibata, S., Katahira, J., Nakagawa, A., Yoneda, Y., and Tsukihara, T. (2009). A high-resolution structure of the pre-microRNA nuclear export machinery. Science *326*, 1275–1279.

Okamura, K., Chung, W.-J., Ruby, J.G., Guo, H., Bartel, D.P., and Lai, E.C. (2008). The Drosophila hairpin RNA pathway generates endogenous short interfering RNAs. Nature *453*, 803–806.

Okamura, K., Hagen, J.W., Duan, H., Tyler, D.M., and Lai, E.C. (2007). The mirtron pathway generates microRNA-class regulatory RNAs in Drosophila. Cell *130*, 89–100.

Orban, T.I., and Izaurralde, E. (2005). Decay of mRNAs targeted by RISC requires XRN1, the Ski complex, and the exosome. Rna *11*, 459–469.

Park, J.-E., Heo, I., Tian, Y., Simanshu, D.K., Chang, H., Jee, D., Patel, D.J., and Kim, V.N. (2011). Dicer recognizes the 5' end of RNA for efficient and accurate processing. Nature *475*, 201–205.

Paroo, Z., Ye, X., Chen, S., and Liu, Q. (2009). Phosphorylation of the human microRNA-generating complex mediates MAPK/Erk signaling. Cell *139*, 112–122.

Phizicky, E.M., and Hopper, A.K. (2010). tRNA biology charges to the front. Genes Dev. *24*,

1832–1860.

Qi, H.H., Ongusaha, P.P., Myllyharju, J., Cheng, D., Pakkanen, O., Shi, Y., Lee, S.W., Peng, J., and Shi, Y. (2008). Prolyl 4-hydroxylation regulates Argonaute 2 stability. Nature *455*, 421–424.

Reinhart, B.J., Slack, F.J., Basson, M., Pasquinelli, A.E., Bettinger, J.C., Rougvie, A.E., Horvitz, H.R., and Ruvkun, G. (2000). The 21-nucleotide let-7 RNA regulates developmental timing in Caenorhabditis elegans. Nature *403*, 901–906.

Ruby, J.G., Jan, C.H., and Bartel, D.P. (2007). Intronic microRNA precursors that bypass Drosha processing. Nature *448*, 83–86.

Saraiya, A.A., and Wang, C.C. (2008). snoRNA, a novel precursor of microRNA in Giardia lamblia. PLoS Pathog. *4*, e1000224.

Sarkies, P., Ashe, A., Le Pen, J., McKie, M.A., and Miska, E.A. (2013). Competition between virus-derived and endogenous small RNAs regulates gene expression in Caenorhabditis elegans. Genome Res. *23*, 1258–1270.

Schnütgen, F., De-Zolt, S., Van Sloun, P., Hollatz, M., Floss, T., Hansen, J., Altschmied, J., Seisenberger, C., Ghyselinck, N.B., Ruiz, P., et al. (2005). Genomewide production of multipurpose alleles for the functional analysis of the mouse genome. Proc. Natl. Acad. Sci. U.S.a. *102*, 7221–7226.

Schnütgen, F., Hansen, J., De-Zolt, S., Horn, C., Lutz, M., Floss, T., Wurst, W., Noppinger, P.R., and Melchner, von, H. (2008). Enhanced gene trapping in mouse embryonic stem cells. Nucleic Acids Res. *36*, e133.

Schwarz, D.S., Hutvagner, G., Du, T., Xu, Z., Aronin, N., and Zamore, P.D. (2003). Asymmetry in the assembly of the RNAi enzyme complex. Cell *115*, 199–208.

Shagin, D.A., Barsova, E.V., Yanushevich, Y.G., Fradkov, A.F., Lukyanov, K.A., Labas, Y.A., Semenova, T.N., Ugalde, J.A., Meyers, A., Nunez, J.M., et al. (2004). GFP-like proteins as ubiquitous metazoan superfamily: evolution of functional features and structural complexity. Mol. Biol. Evol. *21*, 841–850.

Sharp, P.A., Konarksa, M.M., Grabowski, P.J., Lamond, A.I., Marciniak, R., and Seiler, S.R. (1987). Splicing of messenger RNA precursors. Cold Spring Harb. Symp. Quant. Biol. *52*, 277–285.

Shekar, P.C., Naim, A., Sarathi, D.P., and Kumar, S. (2011). Argonaute-2-null embryonic stem cells are retarded in self-renewal and differentiation. J. Biosci. *36*, 649–657.

Siomi, H., and Siomi, M.C. (2010). Posttranscriptional regulation of microRNA biogenesis in animals. Mol. Cell *38*, 323–332.

Stryke, D., Kawamoto, M., Huang, C.C., Johns, S.J., King, L.A., Harper, C.A., Meng, E.C., Lee, R.E., Yee, A., L'Italien, L., et al. (2003). BayGenomics: a resource of insertional mutations in mouse embryonic stem cells. Nucleic Acids Res. *31*, 278–281.

Tabara, H., Sarkissian, M., Kelly, W.G., Fleenor, J., Grishok, A., Timmons, L., Fire, A., and Mello, C.C. (1999). The rde-1 gene, RNA interference, and transposon silencing in C. elegans. Cell *99*, 123–132.

Tabernero, J., Shapiro, G.I., LoRusso, P.M., Cervantes, A., Schwartz, G.K., Weiss, G.J., Paz-Ares, L., Cho, D.C., Infante, J.R., Alsina, M., et al. (2013). First-in-humans trial of an RNA interference therapeutic targeting VEGF and KSP in cancer patients with liver involvement. Cancer Discov *3*, 406–417.

Taft, R.J., Glazov, E.A., Lassmann, T., Hayashizaki, Y., Carninci, P., and Mattick, J.S. (2009). Small RNAs derived from snoRNAs. Rna *15*, 1233–1240.

Tam, O.H., Aravin, A.A., Stein, P., Girard, A., Murchison, E.P., Cheloufi, S., Hodges, E., Anger, M., Sachidanandam, R., Schultz, R.M., et al. (2008). Pseudogene-derived small interfering RNAs regulate gene expression in mouse oocytes. Nature *453*, 534–538.

Teta, M., Choi, Y.S., Okegbe, T., Wong, G., Tam, O.H., Chong, M.M.W., Seykora, J.T., Nagy, A., Littman, D.R., Andl, T., et al. (2012). Inducible deletion of epidermal Dicer and Drosha reveals multiple functions for miRNAs in postnatal skin. Development *139*, 1405–1416.

Timmons, L., Court, D.L., and Fire, A. (2001). Ingestion of bacterially expressed dsRNAs can produce specific and potent genetic interference in Caenorhabditis elegans. Gene *263*, 103–112.

Trombly, M.I., Su, H., and Wang, X. (2009). A genetic screen for components of the mammalian RNA interference pathway in Bloom-deficient mouse embryonic stem cells. Nucleic Acids Res. *37*, e34.

Viswanathan, S.R., Daley, G.Q., and Gregory, R.I. (2008). Selective blockade of microRNA processing by Lin28. Science *320*, 97–100.

Wang, Y., Medvid, R., Melton, C., Jaenisch, R., and Blelloch, R. (2007). DGCR8 is essential for microRNA biogenesis and silencing of embryonic stem cell self-renewal. Nat. Genet. *39*, 380–385.

Wang, Y., Sheng, G., Juranek, S., Tuschl, T., and Patel, D.J. (2008). Structure of the guide-strand-containing argonaute silencing complex. Nature *456*, 209–213.

Watanabe, T., Totoki, Y., Toyoda, A., Kaneda, M., Kuramochi-Miyagawa, S., Obata, Y., Chiba, H., Kohara, Y., Kono, T., Nakano, T., et al. (2008). Endogenous siRNAs from naturally formed dsRNAs regulate transcripts in mouse oocytes. Nature *453*, 539–543.

Wee, L.M., Flores-Jasso, C.F., Salomon, W.E., and Zamore, P.D. (2012). Argonaute divides its RNA guide into domains with distinct functions and RNA-binding properties. Cell *151*, 1055–1067.

Westholm, J.O., and Lai, E.C. (2011). Mirtrons: microRNA biogenesis via splicing. Biochimie *93*, 1897–1904.

Wightman, B., Ha, I., and Ruvkun, G. (1993). Posttranscriptional regulation of the heterochronic gene lin-14 by lin-4 mediates temporal pattern formation in C. elegans. Cell *75*, 855–862.

Xin, H.-B., Deng, K.-Y., Shui, B., Qu, S., Sun, Q., Lee, J., Greene, K.S., Wilson, J., Yu, Y., Feldman, M., et al. (2005). Gene trap and gene inversion methods for conditional gene inactivation in the mouse. Nucleic Acids Res. *33*, e14.

Xu, N., Papagiannakopoulos, T., Pan, G., Thomson, J.A., and Kosik, K.S. (2009). MicroRNA-145 regulates OCT4, SOX2, and KLF4 and represses pluripotency in human embryonic stem cells. Cell *137*, 647–658.

Yang, J.-S., and Lai, E.C. (2011). Alternative miRNA biogenesis pathways and the interpretation of core miRNA pathway mutants. Mol. Cell *43*, 892–903.

Yang, J.-S., Maurin, T., Robine, N., Rasmussen, K.D., Jeffrey, K.L., Chandwani, R., Papapetrou, E.P., Sadelain, M., O'Carroll, D., and Lai, E.C. (2010). Conserved vertebrate mir-451 provides a platform for Dicer-independent, Ago2-mediated microRNA biogenesis. Proc. Natl. Acad. Sci. U.S.a. *107*, 15163–15168.

Yekta, S., Shih, I.-H., and Bartel, D.P. (2004). MicroRNA-directed cleavage of HOXB8 mRNA. Science *304*, 594–596.

Yusa, K., Horie, K., Kondoh, G., Kouno, M., Maeda, Y., Kinoshita, T., and Takeda, J. (2004). Genome-wide phenotype analysis in ES cells by regulated disruption of Bloom's syndrome gene. Nature *429*, 896–899.

Zhang, H., Kolb, F.A., Jaskiewicz, L., Westhof, E., and Filipowicz, W. (2004). Single processing center models for human Dicer and bacterial RNase III. Cell *118*, 57–68.

## Acknowlegement

I would like to thank all my friends and colleagues that have supported me so much during the last years! First of all I want to thank Stefan Ameres for his great supervision and constant support throughout my time in his laboratory. I want to thank all members of the Ameres Lab. Especially Wiebke Wlotzka for the good atmosphere you crated in the lab and your help and advice. I want to thank Valentina Ignatova, Madalena Reimao Pinto and Isabell Grießhammer for being the best possible colleagues. I want to thank as well the Bell, Brennecke, Cochella and Mochizuki groups for the excellent time in the small RNA club, all the services at the VBC campus, especially the biooptics facility for the help at FACS. I want to thank the Zuber group for sharing reagents and expertise and Ulrich Elling for his support with the haploid mouse embryonic stem cells.

# Curriculum Vitae

**Fabian Braukmann**

***26.10.1986**

Schwarzhorngasse 10/7
1050 Vienna
Phone: +43 669 1110 9596
fbnbraukmann@gmail.com

**Education:**

| | |
|---|---|
| Since 03/2011 | Master studies in molecular biology, focus: cell biology, University of Vienna |
| 10/2007 - 02/2011 | Bachelor studies in nutritional sciences, University of Vienna |

**Work Experience**

| | |
|---|---|
| 03/2012 – 04/2012 | Elective laboratory course "Biogenesis of the golgi apparatus", Group Graham Warren, Max F. Perutz Laboratories, Vienna |
| 07/2009 – 09/2009 | ERASMUS Student Mobility Placement: "Proteome analysis in wheat grains", Group Karl H. Mühling, Institute of Plant Nutrition and Soil Science, Christian-Albrechts-Universität, Kiel, Germany |

**Stays abroad:**

| | |
|---|---|
| 01/2007- 10/2007: | Alternative civil service: Care of the children and disabled persons, Centro Social Paroquial de S. Vicente de Paulo", Lisbon, Portugal |

**Awards:**

| | |
|---|---|
| 07/2009 – 09/2009 | ERASMUS Student Mobility for Placements |
| 10/2009 – 02/2010 | ERASMUS Student Mobility for Studies |

**Publications:**

Steinfurth, Dorothee; Zörb, Christian; Braukmann, Fabian; Mühling, Karl-Hermann (2012). **Time-dependent distribution of sulphur, sulphate and glutathione in wheat tissues and grain as affected by three sulphur fertilization levels and late S fertilization.** J Plant Physiol. 1;169(1):72-7.PMID:22070976.

# Supplements

## Supplementary Figure 1.: Enhanced gene-trap conversion, refers to Figure 2.1

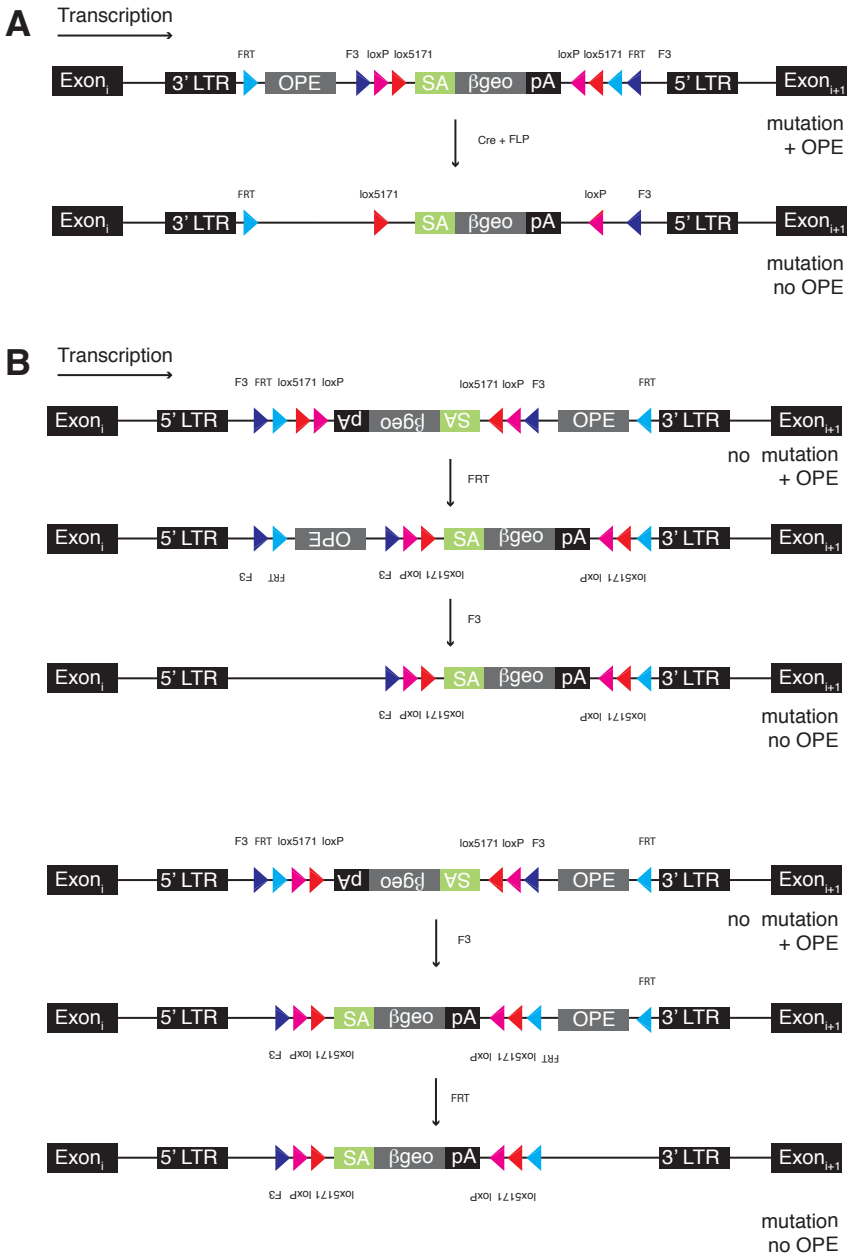

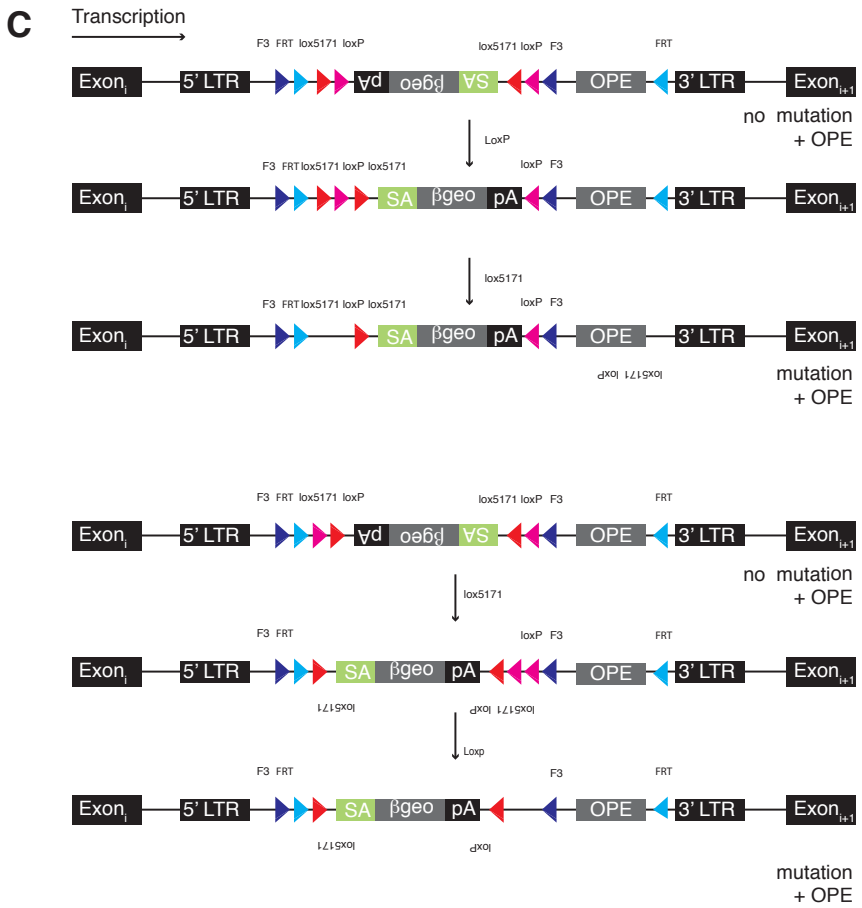


**Supplementary Figure 1** (A) Sense integrated enhanced gene-trap. Gene is mutated and OPE activates transcription. After expression of Cre reombinase and flippase only the OPE sequence is removed.(B) Antisense integration without pertubing function. Flippase expression revert the integration direction via two different reactions and cause a removel of the OPE. (C) Antisense integration without pertubing function. Cre recombinase expression revert the integration direction via two different reactions and cause a perturbed gene function and the OPE sequence is kept. Using this strategy the Drosha mutant mESCs were generated.

## Supplementary Figure 2.: anti-Drosha western blot images, refers to Figure 2.3

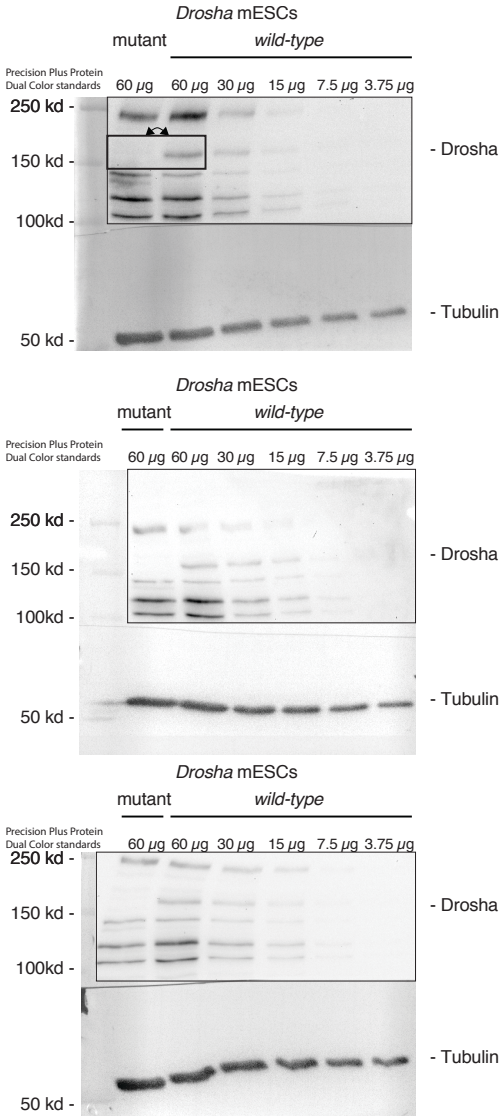


**Supplementary Figure 2** Western Blot analysis of Drosha wt and *Drosha* mutant mESC protein extract (passive lysis buffer 150mM NaCl, 1% TritonZ-100, 50 mM Tris-HCl pH8) 3h at +4 Celsius, centrifugation 20817 g at +4 degree. Protein measurement with Protein Assay Dye Reagent Concentrate. SDS-PAGE 6% at 120 V. Blot on PDFV membrane o/n at +4 degree 30V. Blocking with blocking buffer (5% milk in TBS-T 0.01%). 1. Antibody incubation overnight in blocking buffer (1:1000 anti Drosha (NBP1033349 Novus Biologicals rabbit), 1:200000 anti alpha tubulin (DSHB 12G10 mouse)). 2. Antibody 1:10000 anti rabbit or anti mouse HRP. ImmunStar™ Western C™ Substrate Kit used for detection. Image acquisition and quantification with Molecular Imager® Gel Doc™ XR+ System with Image Lab.

**Supplementary Figure 3.: Norhern Blot images of *Drosha* mutant and *Drosha* wt mESCs, refers to Figure 2.6**

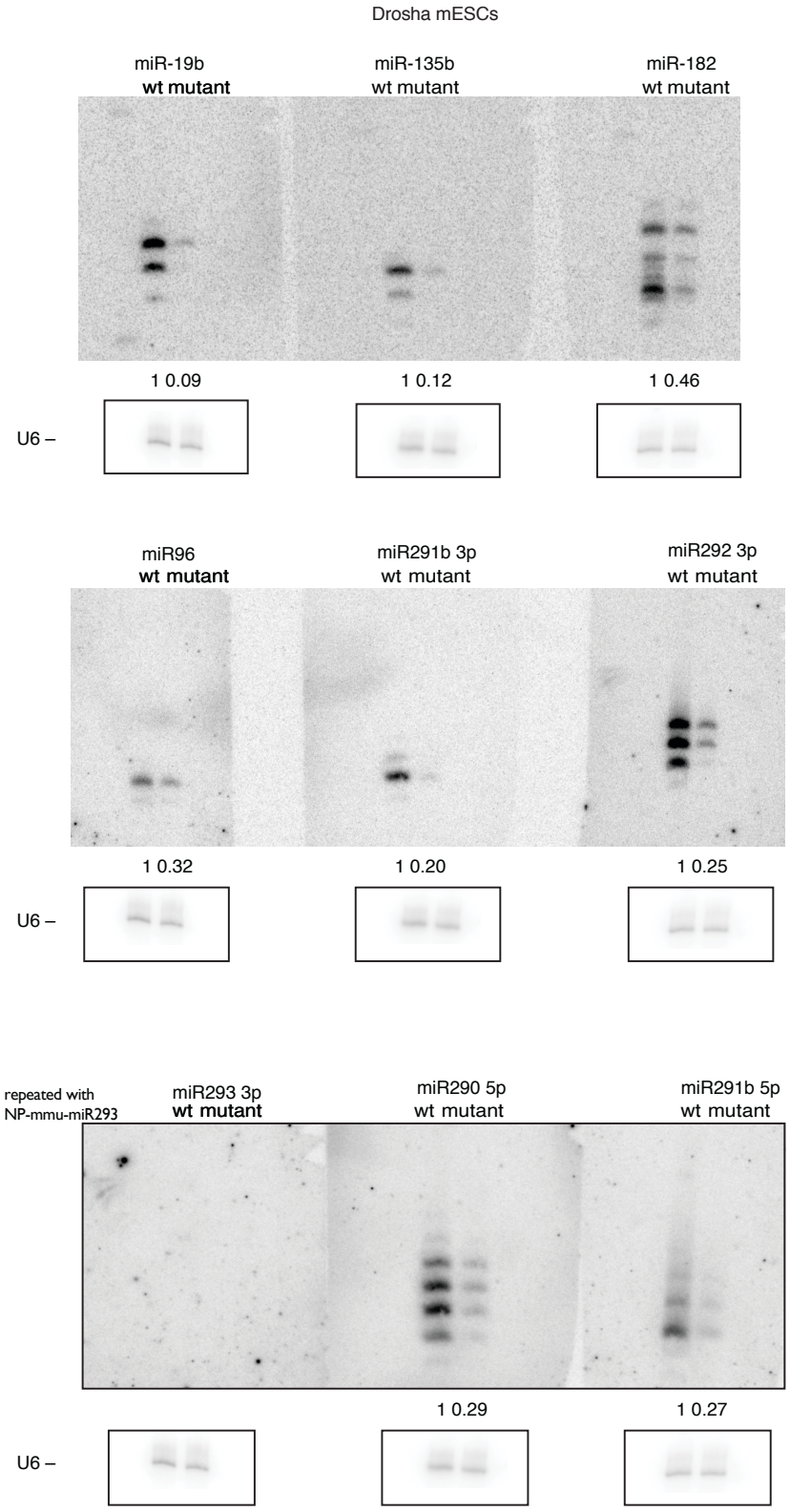

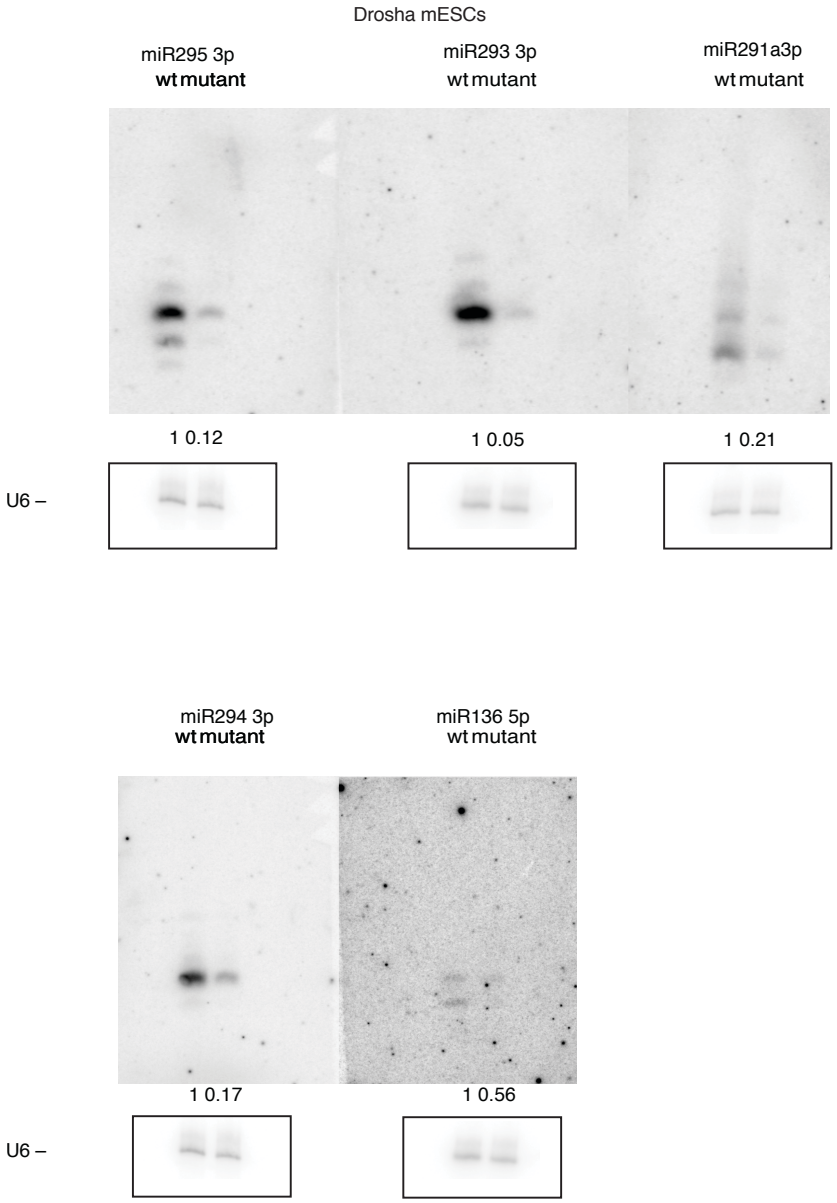


**Supplementary Figure 3** Northern blot analysis of *Drosha* and *Drosha* mutant mESCs. Six $\mu$g total RNA (miRVANA) were extracted. Small RNAs were separated in a 15% denaturing polyacrylamide gel by electrophoresis (80 W, 2 h). Small RNAs (19 – 23 nt) and loading control (U6 snRNP, 106 nt) were transferred under semi dry conditions on Hybond-NX or Amersham Hybond N+ membrane, (20 V, 1 h), respectively. Small RNAs were cross-linked to membrane with EDC solution (60 °C, 1h), whereas UV-crosslinking (2 x 120 mJ, $\lambda$ = 254 nm) was applied for the U6 snRNP loading control. Crosslinked RNA was incubated in church buffer (60 °C, 1 h) and 32P labeled northern probes were hybridized to RNA (37 °C, 12 h) in church buffer. Excessive northern probes were washed away with 1 x SSC washing buffer (3 x, 37 °C, 10 min). Beta radiation was captured on storage phosphor screen and the latent image was scanned at 100 $\mu$m using a Typhoon Trio. The signal intensity was quantified with ImageQuant TL. SmallRNA were normalized to loading control.

## Supplementary Figure 4.: anti-*Dicer* western blot images, refers to Figure 2.7

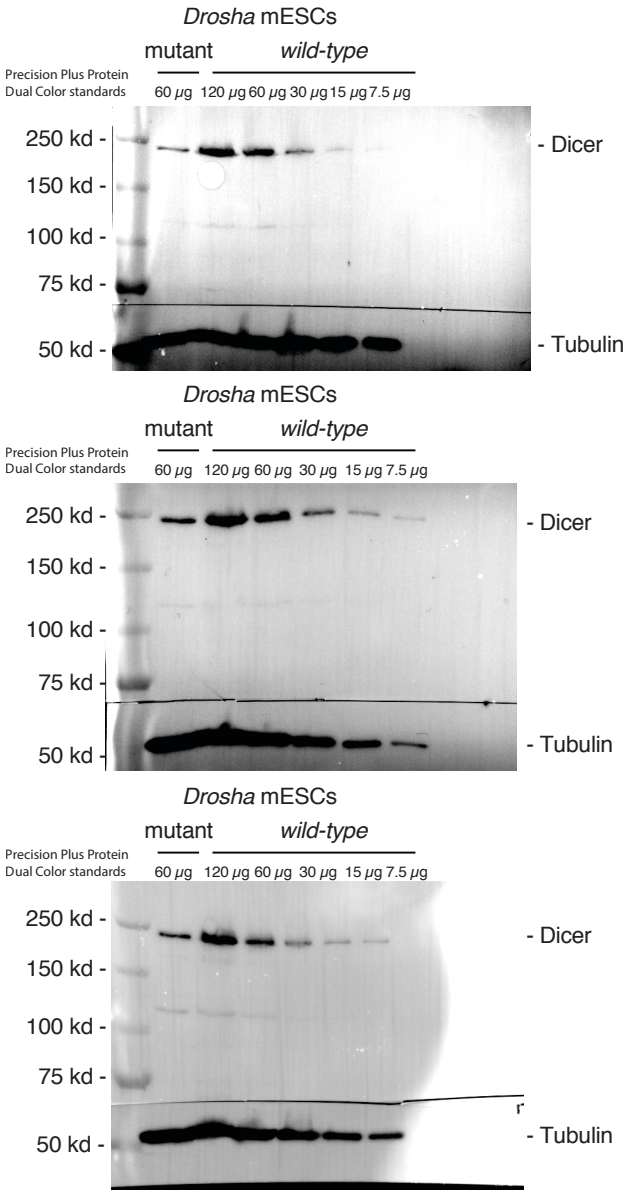


**Supplementary Figure 4** Western Blot analysis of *Drosha* wt and *Drosha* mutant mESC protein extract (passive lysis buffer 150mM NaCl, 1% TritonZ-100, 50 mM Tris-HCl pH8) 3h at +4 Celsius, centrifugation 20817 g at +4 degree. Protein measurement with Protein Assay Dye Reagent Concentrate. SDS-PAGE 6% at 120 V. Blot on PDFV membrane o/n at +4 degree 30V. Blocking with blocking buffer (5% milk in TBS-T 0.01%). 1. Antibody incubation overnight in blocking buffer (1:2000 anti Dicer rabbit (Klaus Rajewsky 2005 gene and development)), 1:200000 anti alpha tubulin (DSHB 12G10 mouse)). 2. Antibody 1:10000 anti rabbit or anti mouse HRP. ImmunStar™ Western C™ Substrate Kit used for detection. Image acquisition and quantification with Molecular Imager® Gel Doc™ XR+ System with Image Lab.

## Supplementary Figure 5.: anti-*Ago2* western blot images, refers to Figure 2.7

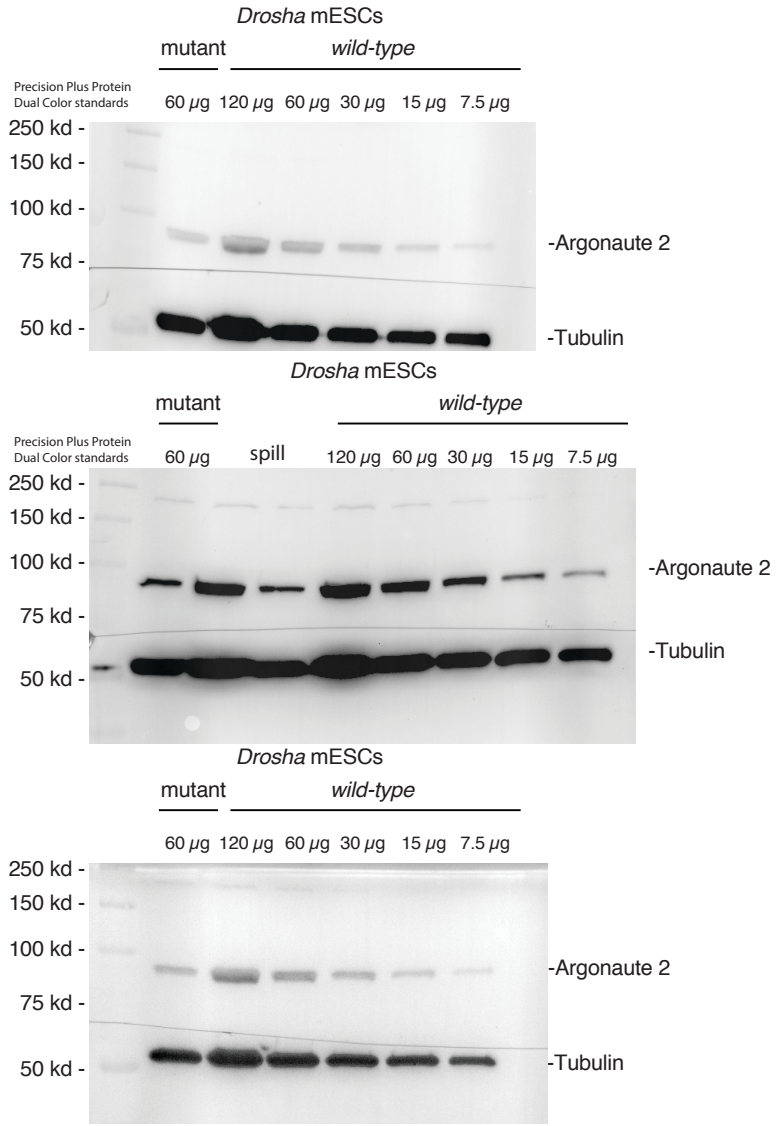


**Supplementary Figure 5** Western Blot analysis of *Drosha* wt and *Drosha* mutant mESC protein extract (passive lysis buffer 150mM NaCl, 1% TritonZ-100, 50 mM Tris-HCl pH8) 3h at +4 Celsius, centrifugation 20817 g at +4 degree. Protein measurement with Protein Assay Dye Reagent Concentrate. SDS-PAGE 6% at 120 V. Blot on PDFV membrane o/n at +4 degree 30V. Blocking with blocking buffer (5% milk in TBS-T 0.01%). 1. Antibody incubation overnight in blocking buffer (1:1000 anti ago2 (C34C6 cell signal rabbit), 1:200000 anti alpha tubulin (DSHB 12G10 mouse)). 2. Antibody 1:10000 anti rabbit or anti mouse HRP. ImmunStar™ Western C™ Substrate Kit used for detection. Image acquisition and quantification with Molecular Imager® Gel Doc™ XR+ System with Image Lab.

## Supplementary Figure 6.: anti-*DGCR8* western blot images, refers to Figure 2.7

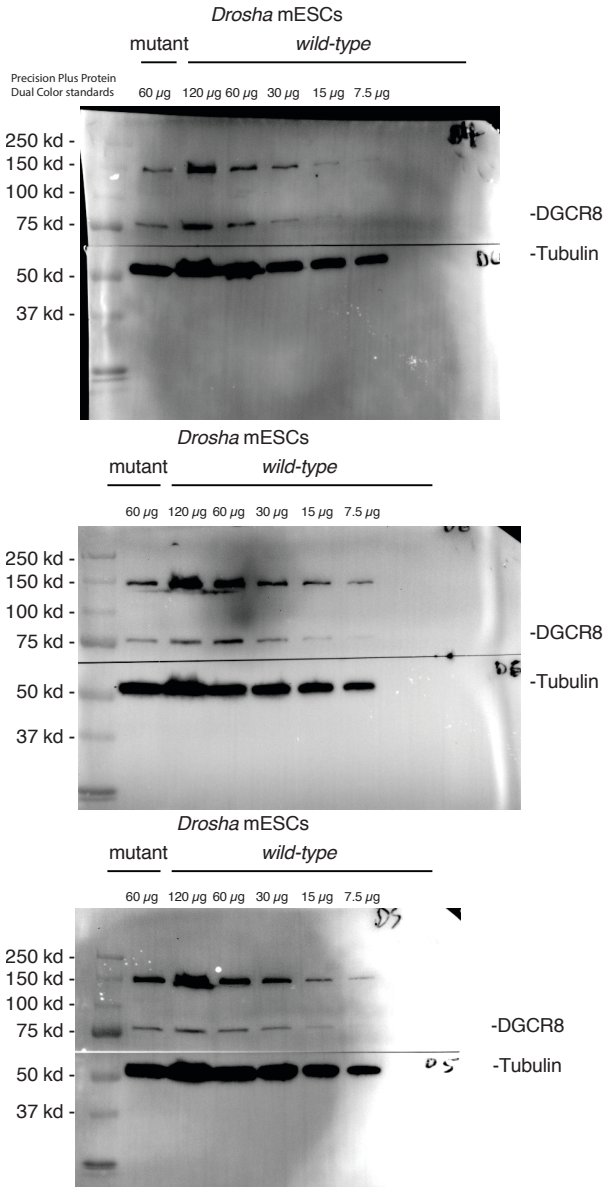


**Supplementary Figure 6** Western Blot analysis of *Drosha* wt and *Drosha* mutant mESC protein extract (passive lysis buffer 150mM NaCl, 1% TritonZ-100, 50 mM Tris-HCl pH8) 3h at +4 Celsius, centrifugation 20817 g at +4 degree. Protein measurement with Protein Assay Dye Reagent Concentrate. SDS-PAGE 6% at 120 V. Blot on PDFV membrane o/n at +4 degree 30V. Blocking with blocking buffer (5% milk in TBS-T 0.01%). 1. Antibody incubation overnight in blocking buffer (3:10000 anti DGCR8 goat Thermo scientific PA5-18614, 1:200000 anti alpha tubulin (DSHB 12G10 mouse)). 2. Antibody 1:10000 anti goat or anti mouse HRP. ImmunStar™ Western C™ Substrate Kit used for detection. Image acquisition and quantification with Molecular Imager® Gel Doc™ XR+ System with Image Lab.